

# Mapping of human and macaque sensorimotor areas by integrating architectonic, transmitter receptor, MRI and PET data

KARL ZILLES<sup>1</sup>, GOTTFRIED SCHLAUG<sup>2</sup>, MASSIMO MATELLI<sup>3</sup>, GIUSEPPE LUPPINO<sup>3</sup>, AXEL SCHLEICHER<sup>1</sup>, MEISHU QŪ<sup>1</sup>, ANDREAS DABRINGHAUS<sup>1</sup>, RÜDIGER SEITZ<sup>2</sup> AND PER E. ROLAND<sup>4</sup>

<sup>1</sup>Brain Research Institute and <sup>2</sup>Department of Neurology, University of Düsseldorf, Germany; <sup>3</sup>Istituto di Fisiologia Umana, Università di Parma, Parma, Italy; and <sup>4</sup>Division of Human Brain Research, Department of Neuroscience, Karolinska Institute, Stockholm, Sweden

(Accepted 7 March 1995)

---

## ABSTRACT

The human and macaque sensorimotor cortex was subdivided into numerous areas by a correlative analysis based on cytoarchitectonics, myeloarchitecture and the distribution of transmitter receptors. Receptor densities and laminar distribution patterns differ not only between motor and somatosensory regions, but also between different areas within these regions of the cortex. Changes in receptor distribution often match architectonically defined borders. Receptor findings provide new criteria for a more detailed mapping in the human brain which cannot be achieved by cytoarchitectonic analysis alone. Morphological data on these areas were integrated with functional data from positron emission tomography (PET) on the basis of a recently developed computerised brain atlas. The central sulcus marks the border between (1) the agranular motor cortex with a generally low density of glutamatergic, muscarinic, GABAergic and serotonergic receptors, and (2) the granular somatosensory cortex with higher densities of these receptors. Rostral to the primary motor cortex, 2 isocortical areas are found on the mesial cortex which probably represent the functionally defined supplementary motor areas (SMA) SMA-proper (caudally) and pre-SMA (rostrally). Below SMA-proper the areas 24d (macaque) and the caudal cingulate motor area cmc (human) are located in the cingulate sulcus. Both regions correspond to the 'posterior cingulate motor areas' of recent PET studies and to the posterior part of the agranular cingulate cortex of architectonic studies. Below pre-SMA the area 24c (macaque) and the rostral cingulate motor area cmr (human) are located in the cingulate sulcus; they correspond to the 'anterior cingulate motor areas' of recent PET observations and to the anterior part of the agranular cingulate cortex of architectonic studies. Homologous sensorimotor areas can be defined in both species on the basis of common architectonic features.

*Key words:* Motor cortex; somatosensory cortex; receptor autoradiography; cytoarchitectonics; myeloarchitectonics.

---

## INTRODUCTION

More than 130 years ago the cerebral cortex was demonstrated to be a centre of motor activity by Jackson's (1863, 1870) careful clinical observations of patients with focal epilepsy or stroke. Fritsch & Hitzig (1870), Ferrier (1866) and Grünbaum & Sherrington (1903) identified a region surrounding the central sulcus in primates and a comparable region in nonprimate mammals as the sensorimotor cortex.

They had already concluded by critically discussing the techniques available at the time, that this region may be subdivisible into functionally different areas. Krause (1911) and Foerster (1936) elicited motor responses and somatosensory sensations by stimulating a large cortical region in front of and behind the central sulcus in human subjects. They published detailed maps illustrating the somatotopy of different motor activities in the precentral gyrus.

The later studies by Penfield & Rasmussen (1950)

expanded our knowledge on the representation of motor functions in the human cortex considerably. These authors suggested that the motor representation might be organised as a 'motor homunculus' representing a schematic summary of the somatotopic aspects of their stimulation studies. Although they always emphasised that the homunculus represents motor activities and not muscles, this scheme led to conceptual confusions, because the homunculus was interpreted by many successors in original reports and in textbooks to represent anatomical entities such as muscles or fingers. Consequently, the observation, e.g. that 1 finger is represented several times in the area covered by the motor homunculus, seemed to be puzzling and a challenge for the original scheme.

Recent hypotheses (Lemon, 1988; Schieber, 1990) again emphasised the *functional* aspects of maps of motor representations. According to these hypotheses the motor cortex programs movements and thus the multiple representation of a single finger means that it can be activated from different locations in the motor cortex, depending upon the complex patterns of movement in which it is involved. Clearly the homunculus scheme also includes anatomical somatotopy, since under standard conditions the hand is never represented, e.g. in the leg area of the cortex. The various functional and anatomical aspects of movement are therefore the driving forces behind the organisation of the sensorimotor cortex into numerous areas. Considering the technical restrictions in spatial resolution and specificity of electrophysiological, PET or functional MR imaging, the anatomical analysis of sensorimotor areas is necessary in order precisely to locate PET and MR data or interpret the structural features behind functional observations.

Cytoarchitectonic and myeloarchitectonic studies by Brodmann (1903, 1905/06, 1909), Campbell (1905), Cecile and Oscar Vogt (1910, 1919, 1926) and von Economo & Koskinas (1925) showed that the functional inhomogeneity of the sensorimotor region is paralleled by a structural inhomogeneity. Although their maps differ in many aspects, they all have one feature in common: the central sulcus subdivides the adult sensorimotor cortex into two large regions: (1) a caudally located, 6-layered granular cortex with a clearly delineable layer IV and (2) a more rostrally located, 5-layered agranular cortex lacking a layer IV.

The agranular region represents the motor cortex. It covers the posterior half of the frontal lobe and is bordered rostrally by the granular, 6-layered prefrontal cortex. The agranular part of the isocortex is delineated from the adjoining allocortex on the mesial

surface of the hemisphere by the cingulate sulcus, where Brodmann's area 24 is located. Brodmann (1903, 1905/06, 1909) further subdivided the agranular cortex into an area 4, primary motor cortex, and a rostrally adjoining premotor area 6, secondary motor cortex. Area 4 is found mainly in the rostral wall of the central sulcus and encroaches on the free surface of the precentral gyrus in its dorsal part. Area 6 was further parcellated by Vogt & Vogt (1919) into several subareas, 6 $\alpha$ , 6 $\beta$ , 6 $\alpha$  and 6 $\beta$ . Brodmann (1909) subdivided the granular cortex of the postcentral gyrus into the primary somatosensory areas 3, 1 and 2 (rostrocaudal sequence), which all display a layer IV (koniocortex). Layer IV appears to be less densely packed in the caudally adjoining parietal 'association' regions, which contain areas 5 and 7 of Brodmann, than in the 3 areas immediately in front of them.

Despite the rather good agreement on the principal subdivision into agranular motor and granular somatosensory regions, it becomes evident when comparing the maps of the different authors, that the positions of the borders between the areas vary considerably (for review see Zilles 1990). Discrepancies are particularly large for the border between areas 4 and 6. It is not yet clear to what extent these inconsistencies are due to methodological problems inherent to the highly observer-dependent evaluation of conventional cytoarchitectonic and myeloarchitectonic sections, or if they reflect individual variability in the size of cortical areas. The importance of reliable and detailed maps becomes even more evident if the experimental findings in subhuman primates, the clinical observations after lesions in different locations and the PET studies carried out during various motor and somatosensory tasks are to be compared with the architectonic parcellations. All these functional investigations revealed many more areas than shown in the classical architectonic maps.

Analysis of cytoarchitectonic and myeloarchitectonic specimens should therefore be based on more reliable criteria than those achieved by pure visual inspection. They should also be supplemented by more functionally oriented observations. Since functional differences between cortical areas are at least partially reflected in the distribution patterns of transmitter receptors, we have used quantitative *in vitro* receptor autoradiography for characterizing cortical, especially visual areas (Zilles, 1991; Zilles & Schleicher, 1993). In summary, the parcellation of the human sensorimotor cortex is still far from being complete and does not yet present an areal pattern integrating functional and anatomical findings.

Our present results from quantitative architectonic and receptor autoradiographic studies on postmortem brains extend our knowledge about the precise topography and positional variability, the architecture and neurochemical characteristics of the different areas of the human and macaque sensorimotor cortex. PET data have been added by integrating the data from the different approaches and modalities on the basis of a computerised brain atlas (Roland & Zilles, 1994). The following questions will be considered. (1) Is it possible to define the structural features of the different sensorimotor areas objectively by *quantitative* architectonic analyses? (2) Do the patterns of transmitter receptor distribution differ among the motor and somatosensory areas? (3) Are the cyto-, myelo- and receptorarchitectonic features of the human sensorimotor areas comparable with those of the macaque?

#### MATERIAL AND METHODS

##### *Architectonic techniques*

Nissl and myelin-stained serial sections (20  $\mu\text{m}$ ) through formalin or Bodian-fixed and paraffin-embedded total hemispheres or brains from 10 human subjects of both sexes were available for architectonic observations. Three of these brains were scanned with a 3D flash sequence in an MR scanner before embedding. The MR images were used for correcting the inevitable histological shrinkage and distortions in the Nissl and myelin-stained sections from these brains (Schormann et al. 1993, 1995), for 3D reconstructions, for the spatially correct transfer of data into the computerised brain atlas (Roland & Zilles, 1994; Roland et al. 1994) and for studying intersubject variability in cortical maps. Quantitative cytoarchitectonic and myeloarchitectonic studies were performed according to previously published techniques (Schleicher et al. 1986). In summary, cell-packing densities and densities of myelinated fibres were measured in Nissl and myelin-stained sections, respectively. Both types of measurements were carried out with an IBAS 2000 image analyser using an automated scanning procedure. The results were presented as profile curves extending from the pial surface (cortical depth 0%) to the cortex/white-matter border (cortical depth 100%).

##### *Quantitative in vitro receptor autoradiography*

For quantitative receptor autoradiography, unfixed tissue blocks from 5 human brains and an entire

hemisphere were frozen in isopentane at  $-50^\circ\text{C}$  and stored at  $-70^\circ\text{C}$  until sectioning. There was no history of neurological or psychiatric disease. Three macaque brains were processed in the same manner. The animals were killed with an overdose of barbiturate. After serial sectioning (10–30  $\mu\text{m}$  thickness) with a cryostat microtome for large sections in coronal, horizontal (axial) and sagittal planes, the tissue was processed according to standard procedures for receptor autoradiography (Zilles et al. 1988, 1991a, b, 1993, 1995). Cholinergic muscarinic M1 and M2, GABA<sub>A</sub>, serotonergic 5-HT<sub>1</sub> and 5-HT<sub>2</sub>, noradrenergic  $\alpha_1$  and  $\alpha_2$  receptors, L-glutamate binding sites, glutamatergic NMDA, AMPA and kainate receptors were labelled with the respective tritiated ligands ( $[^3\text{H}]$ pirenzepine,  $[^3\text{H}]$ oxotremorine-M,  $[^3\text{H}]$ -muscimol,  $[^3\text{H}]$ 5-hydroxytryptamine creatinine sulphate,  $[^3\text{H}]$ ketanserin,  $[^3\text{H}]$ prazosin,  $[^3\text{H}]$ UK 14304,  $[^3\text{H}]$ L-glutamic acid,  $[^3\text{H}]$ MK801 in the presence of unlabelled spermidine and glycine,  $[^3\text{H}]$ AMPA,  $[^3\text{H}]$ -kainate). In addition, alternating sections were Nissl and myelin stained. After 6–12 wk exposure of the sections together with brain paste or plastic standards of known radioactivity (to correct for the nonlinear relationship between optical densities and concentrations of radioactivity) against Hyperfilm (Amersham), the regional distributions of receptors were visualised and measured with an IBAS 2000 image analyser (Schleicher & Zilles, 1988). With this procedure, specific receptor binding can be measured in fmol/mg protein and colour-coded images of regional and laminar distribution patterns compiled.

After identifying the areal borders in the Nissl-stained sections, they were copied onto prints of contrast enhanced images of autoradiographs displaying the distribution patterns of the various receptors. Since the autoradiographic sections were always located very close to the Nissl-stained sections, no major shifts in the positions of the cytoarchitectonically defined borders needed to be taken into account. In some cases it was not possible to define a specific areal border reliably on the basis of cytoarchitecture or myeloarchitecture; here we used the receptor autoradiographs for delineation. In other cases, in which the border of a larger area could be defined at exactly the same location in cyto-, myelo- and receptor architectonic observations, the larger area could be further subdivided on the basis of receptor data.

Observations on postmortem human brains and the MR and PET studies were performed with the understanding and consent of each subject and conform with the Declaration of Helsinki.

RESULTS

*Cytoarchitectonics and myeloarchitecture of the human and macaque sensorimotor cortex*

**Human sensorimotor cortex.** The absolute thickness of the cortex in the motor region (areas 4 and 6) is about double that of the somatosensory region (areas 3, 1 and 2). The proportions between the widths of supragranular (I–III(IV)) and infragranular (V–VI) layers show clear differences between both regions with ratios of approximately 1:2 for all motor and 2:1 for all somatosensory areas (Fig. 1a). The functional difference between motor and somatosensory regions is therefore reflected in simple measurements of cortical or laminar dimensions. The relative widths of the single layers also vary between the different motor and somatosensory areas (Fig. 1b). However, the variations between the different areas within a region, either motor or somatosensory, are much smaller than between the two regions. Therefore, the measurement

of the widths of single layers is not an adequate tool for parcellation of the different motor or somatosensory areas, but it is very effective for separating motor from somatosensory regions.

The isocortex in the anterior bank of the central sulcus displays the typical architectonic features of Brodmann's area 4, i.e. agranular (lack of layer IV) cortex and presence of Betz cells in layer V (Fig. 2d). These cells tend to form clusters, which are more frequently found deep in the sulcus than in the more superficial parts of the bank or on the free surface of the precentral gyrus. The part of the precentral gyrus completely buried in the central sulcus corresponds to the posterior part of Brodmann's area 4; it is therefore called subarea 4p. The more rostrally located part of the anterior bank and the superficially exposed part represents the anterior portion of area 4 and is called here subarea 4a. Since the distance between single Betz cells increases towards subarea 4a, the border between area 4 and the rostrally adjoining part of the agranular cortex (area 6 of Brodmann) is sometimes difficult to define precisely on the basis of the Betz cell criterion alone. By contrast, the posterior border of area 4 is visible by the incipient layer IV (Jones & Porter, 1980) in the caudally neighbouring area 3a of the somatosensory cortex (Fig. 2c). Area 3a is followed caudally by area 3b showing all characteristics of a typical primary sensory area, especially a well developed layer IV (Fig. 2b). Areas 2 (not shown) and 1 (Fig. 2a) are difficult to differentiate from each other on the basis of pure visual inspection of Nissl or myelin-stained sections. The measurement of packing densities of perikarya or myelinated fibres objectifies and extends the above described distinctions between sensorimotor areas. The densities were measured from the pial surface to the border between cortex and white matter. About 80–180 measuring fields in one brain were the basis for the curves shown in Figures 3–7. The standard deviations of the profile curves are less than 10%. The resulting profile curves allow a quantitative characterisation of the architectonic features in the different areas. The maximal cortical widths and the mean cell packing densities or densities of myelinated fibres (grey level index GLI) of the different areas were standardised to 100% (cortical depth in percentages and GLI in percentages, respectively), in order to compare areas of different absolute dimensions and cell or myelin densities directly (Figs 3–9). Area 6 reaches a maximal cell packing density in upper layer V, whereas areas 4a and 4p show maxima in the middle of layer V and in the upper part of layer VI (Figs 3–4). The somatosensory area 1 reaches its maximal cell packing

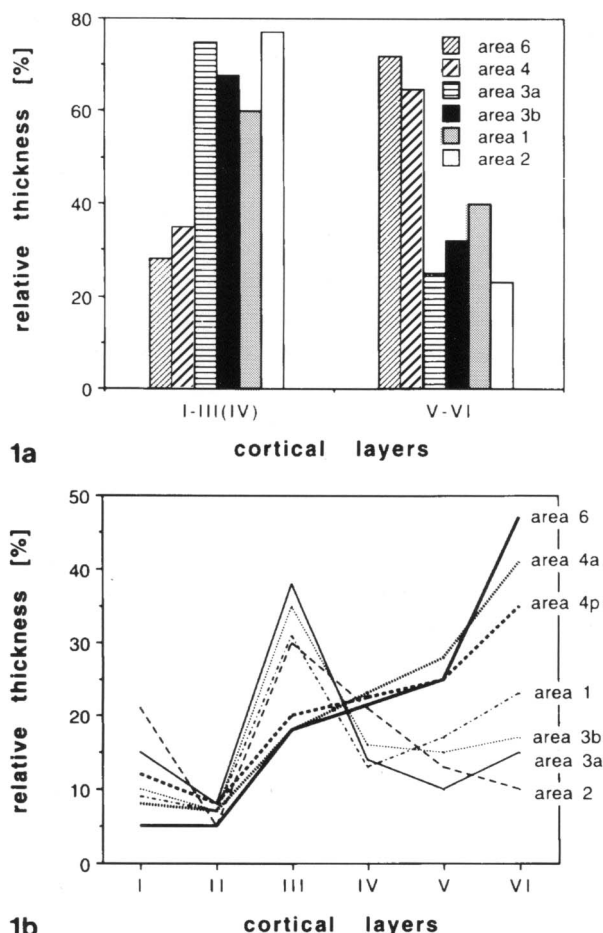


Fig. 1. Relative thicknesses of supragranular and infragranular (a) and single (b) layers in 6 different sensorimotor areas of the human cortex. The relative thicknesses are calculated as percentages of the total thickness (100%) of the respective area.



density in the middle of the cortex (upper layer IV), area 3b in the centre of layer IV and area 2 in the lower part of layer IV (Fig. 5). Area 3a has a second maximum in layer V, which reflects – together with the maximum in layer IV – its transitional character between the motor and somatosensory regions (Jones & Porter, 1980). In addition, the extremely high absolute cell packing density in area 3b separates it from the rostrally adjoining area 3a and the caudally adjoining area 1. The quantitative differences in cytoarchitecture between the motor and somatosensory regions are shown in Fig. 6. The relative density of myelinated fibres in the motor areas increases from a minimum in lower layer I and layer II to layer V (Fig. 7a). Area 4p has a higher myelin density in layers V–VI than areas 4a or 6. This underlines the difference between the subareas 4a and 4p of the primary motor cortex and can be even more clearly demonstrated by receptor labelling (see below). All somatosensory areas show a first clear maximum in myelin density in layer IV, which reflects the external stripe of Baillarger, and the areas 3b and 1 a second maximum in lower layer V, which reflects the internal stripe of Baillarger (Fig. 7b). The 3 primary somatosensory areas (3b, 2 and 1) show – in contrast to the transitional area 3a – a further increase in myelin density from upper layer IV to the cortex/white matter border. Especially the clearly measurable stripes of Baillarger delineate the somatosensory region from the motor region in myelin-stained sections.

Comparable measurements of the cytoarchitectonics and myeloarchitecture of the mesial agranular cortex, including the cingulate areas, are still lacking. We have therefore relied on the classical descriptive approach for the cyto- and myeloarchitectonic parcellation of this region. Since the areal borders found in the receptor studies (see below) match the borders defined by visual inspection of Nissl and myelin-stained sections, the results provided by the classical approach were confirmed by an independent and quantitative method. The mesial part of area 6, which may represent the supplementary motor area (SMA) of Penfield & Rasmussen (1950), differs from the lateral part of area 6, the putative premotor cortex, because of its slightly higher mean density. The caudal part of the mesial area 6 (Fig. 2g) can be distinguished from the respective lateral part (Fig. 2e) by an increased cell density in its lower layer III and Va. This caudal mesial area 6, the putative SMA-proper (see below) can be further delimited from the rostral mesial area 6, the putative pre-SMA (Fig. 2h), by the more pronounced lamination and the clearer

demarcation of layer III from layer V in the latter area (Fig. 2j). The pre-SMA is bordered laterally by the rostral part of Brodmann's area 6, which is probably area 6a $\beta$  (Fig. 2f) of Vogt & Vogt (1919).

Several cingulate areas, which may represent the cingulate motor areas of recent PET studies, are also definable in our architectonic sections. The human anterior cingulate cortex (areas 24 and 32 of Brodmann) is agranular and differs because of this from the dysgranular to granular posterior cingulate cortex (areas 23 and 31 of Brodmann). The primate anterior cingulate region shows a gradual change in its cytoarchitecture from a true isocortical (area 32 of Brodmann), through a proisocortical (dorsal part of area 24 of Brodmann), a periallocortical (lower part of area 24 of Brodmann) and finally to a true allocortical structure (area 33 of Brodmann). The dorsal part of area 24 in the cingulate sulcus can be further subdivided into a rostral area 24c and an adjoining caudal area 24d. Area 24d contains an architectonically distinct subarea (cmc1), which is characterised by very large pyramidal cells in layer V (Fig. 2i). These cells are smaller in the more rostral part of area 24d, which is therefore termed cmc2 (Fig. 2j). Area 24c is apparently also not a single field, but for the definition of subareas further cytoarchitectonic studies are necessary. Area cmc2 of 24d can be delineated from area 24c by the thicker layer V and an intermediate band of lower cell density within layer V in the latter area (Fig. 2l). Area 24c can easily be delineated from the ventrally adjoining cingulate proisocortex (area 24b) by the clear separation of layers V and VI in 24b (Fig. 2k), which leads to a more 'periallocortical' appearance of area 24b.

*Macaque sensorimotor cortex.* The cytoarchitecture of the macaque frontal agranular cortex has already been described in detail by Matelli et al. (1991). Only the most important criteria for areal parcellation and comparison with the human cortex will be repeated here. Area 3b shows an extremely dense packing of perikarya in layer IV and a slightly lower density in layer III. It is a koniocortical area with the typical appearance of the primary somatosensory cortex in primates. The rostrally adjacent area 3a has an incipient layer IV, a relatively high cell density in layer Va and a clear demarcation of layer V from layer VI. A few giant pyramidal cells in layer Vb are occasionally found in the border region to area 4.

Area 4 (area F1 of Matelli et al. 1991) is characterised by the absence of layer IV, the presence of Betz cells arranged in multiple rows in layer Vb and by poor lamination (Fig. 2m).

The caudal and laterodorsal part of area 6 (area F2

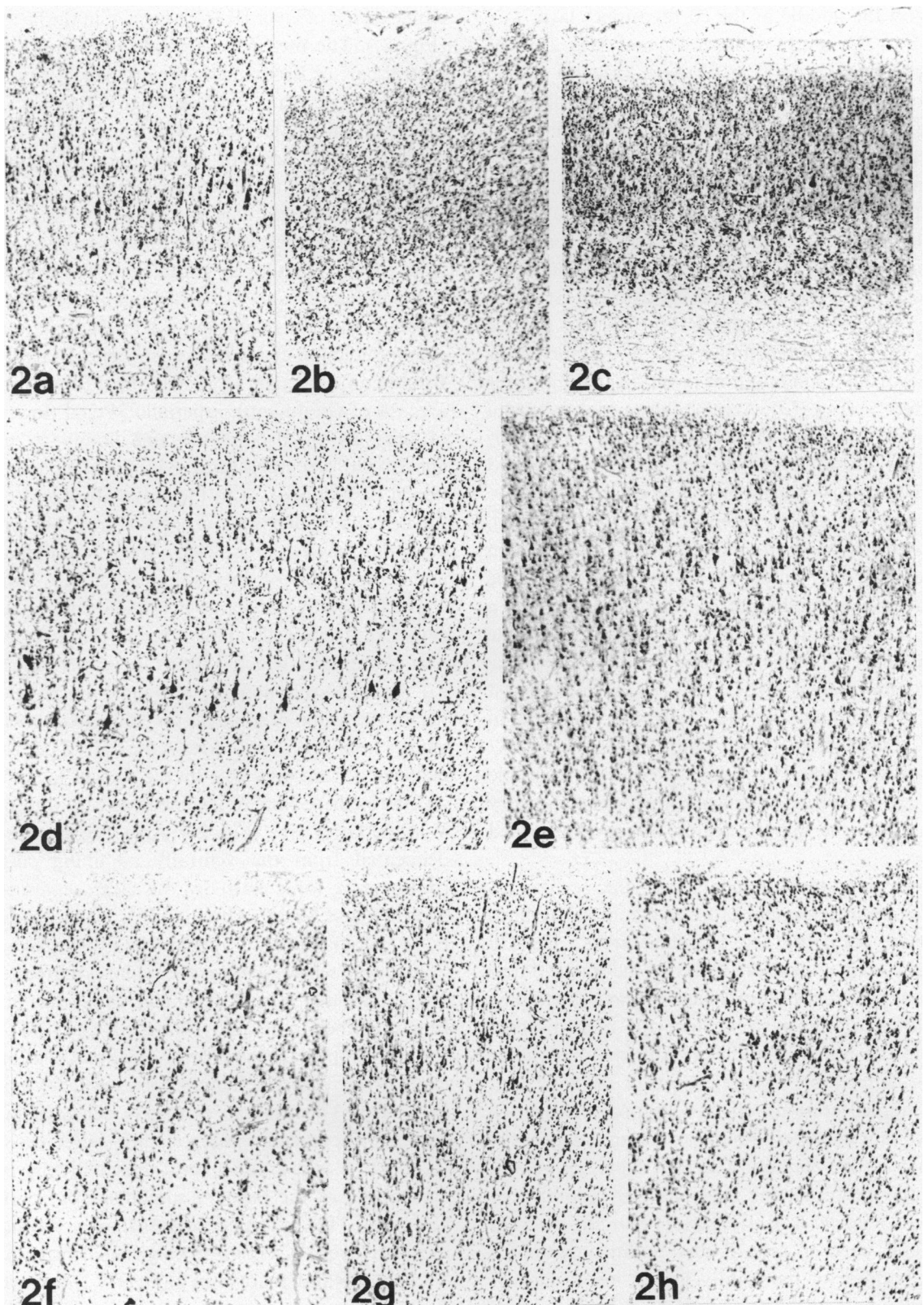


Fig. 2 (a-h). For legend see opposite.

of Matelli et al. 1991) contains medium-sized pyramids at the border between layers III and V (Fig. 2n). A few scattered giant pyramidal cells can

occasionally be found in layer V. The lamination of area F2 is also poorly developed.

The posteromesial part (Fig. 2o) of area 6 (area F3

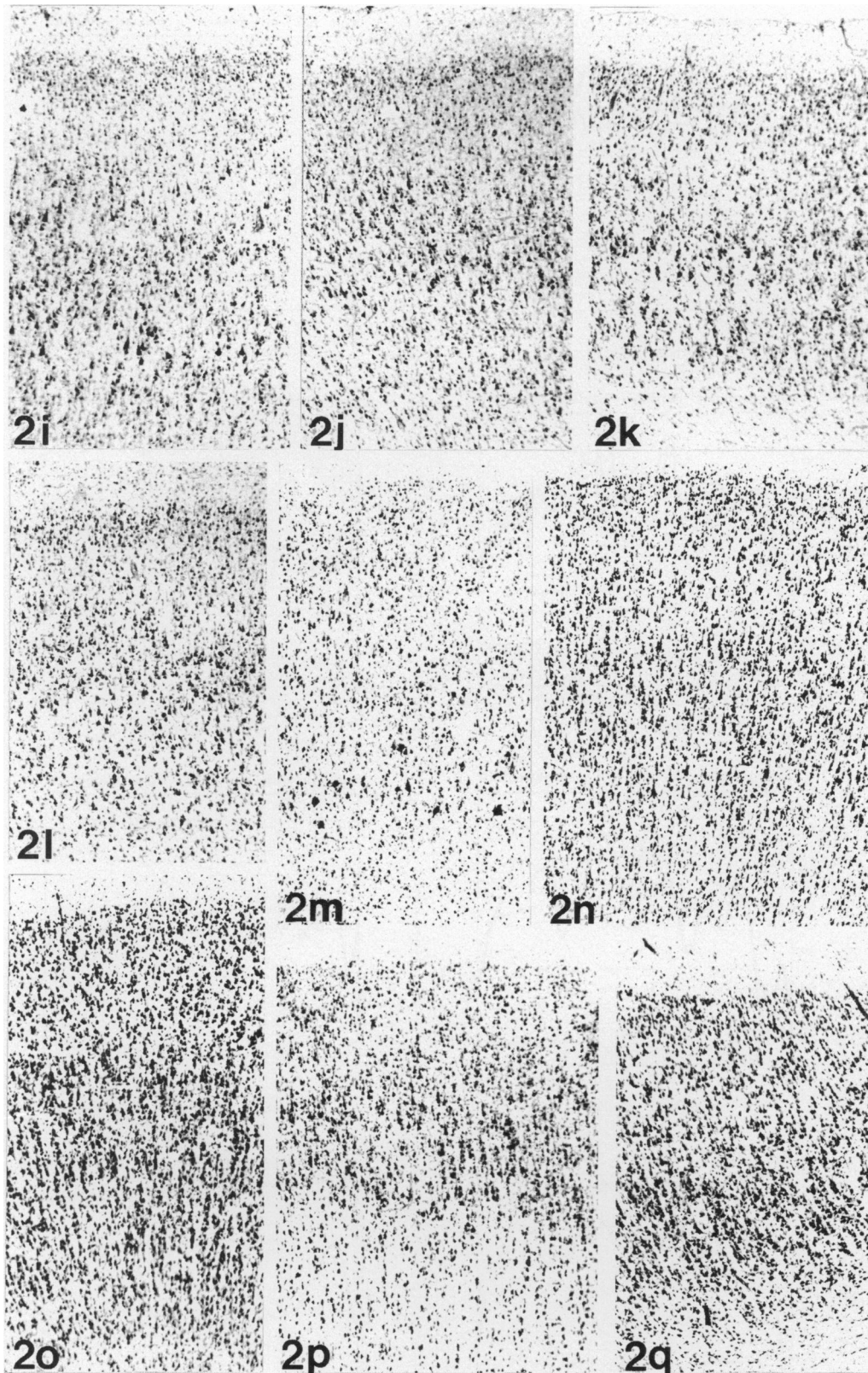
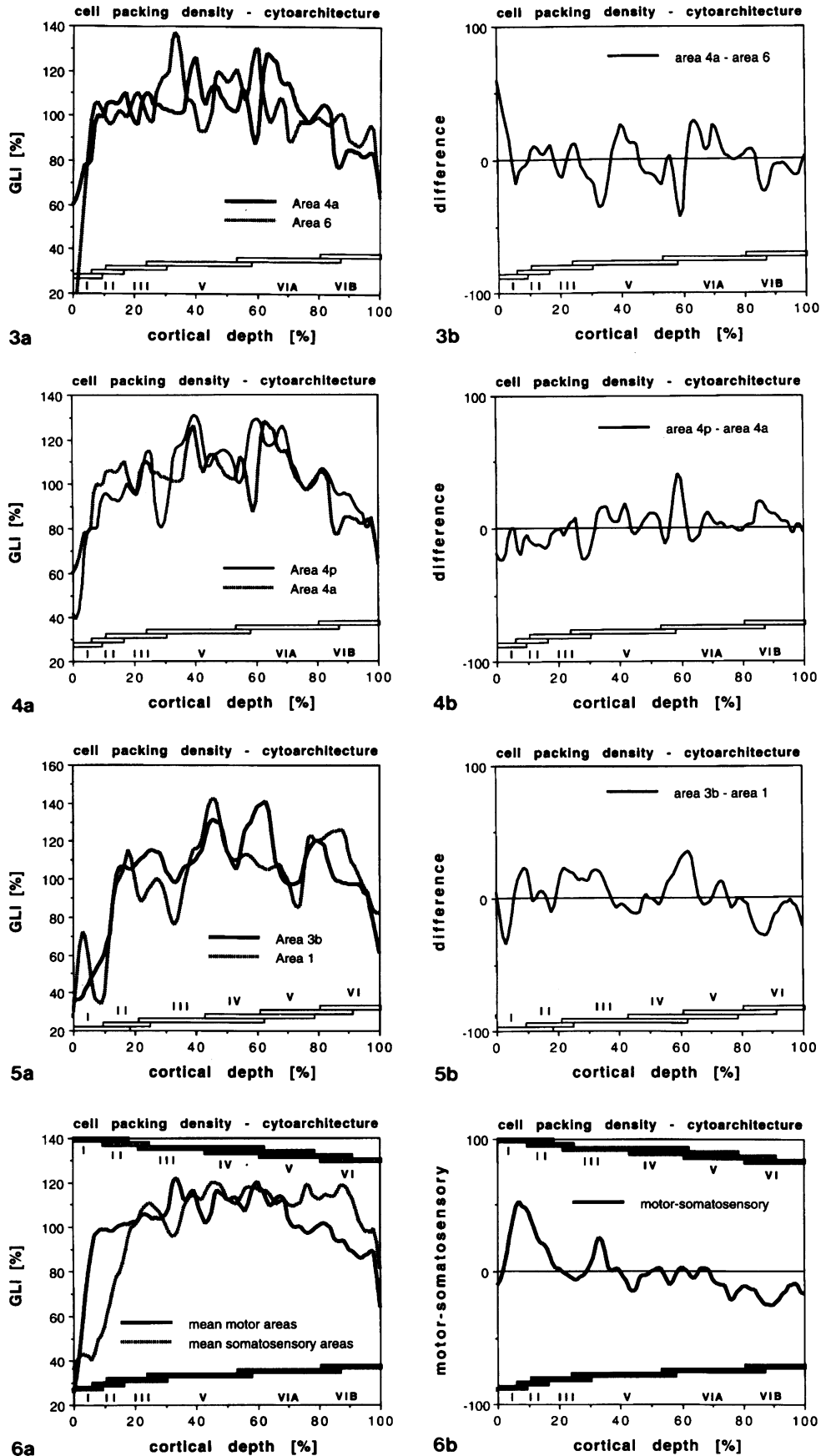


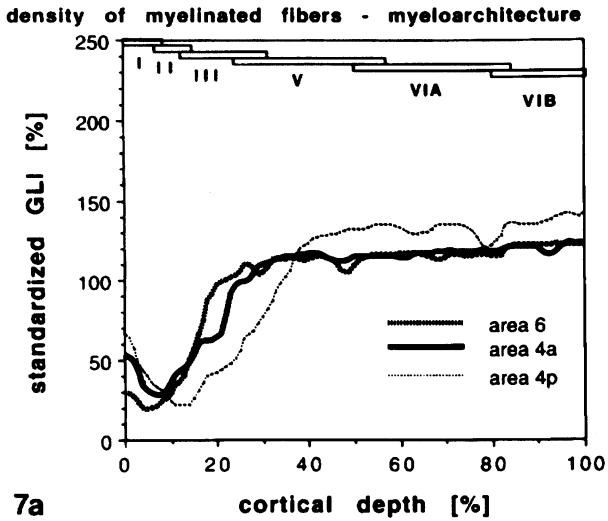
Fig. 2. Cytoarchitectural appearance of Brodmann's areas 1 (a), 3b (b), 3a (c), 4 (d), 6 $\alpha\alpha$  (e), 6 $\alpha\beta$  (f), caudal mesial area 6 (g), rostral mesial area 6 (h), cmc1 (i), cmc2 (j), 24b (k) and cmr (l) in the human cortex. Panels m–q show the comparable areas in the macaque cortex (F1, m; F2, n; F3, o; F6, p; 24d, q).

of Matelli et al. 1991) shows increased cell density in the lower part of layers III and in layer Va. Large cells are present in a single row in the caudal part of F3.

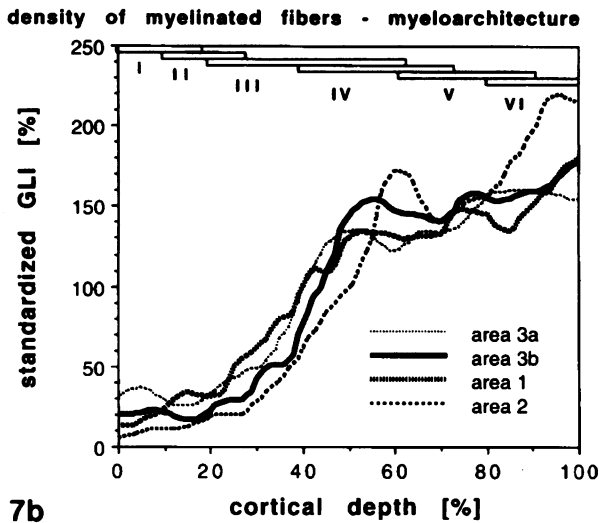
The lamination is poor and layer VI appears more densely packed than layer Vb. The rostromesial part (Fig. 2p) of area 6 (area F6 of Matelli et al. 1991)



Figs 3–6. Profile curves through the cortex of different sensorimotor areas and subareas in Nissl-stained sections as quantitative descriptions of cytoarchitecture. The x-axis shows the position of each measurement relative to the pial surface, whereby the total cortical thickness of each area is defined as 100% (pial surface = 0%; cortex/white matter border = 100%). The y-axis shows the packing density of perikarya



7a

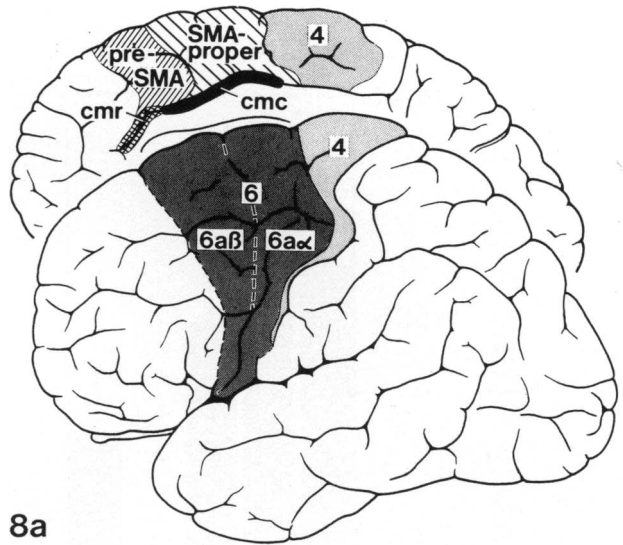


7b

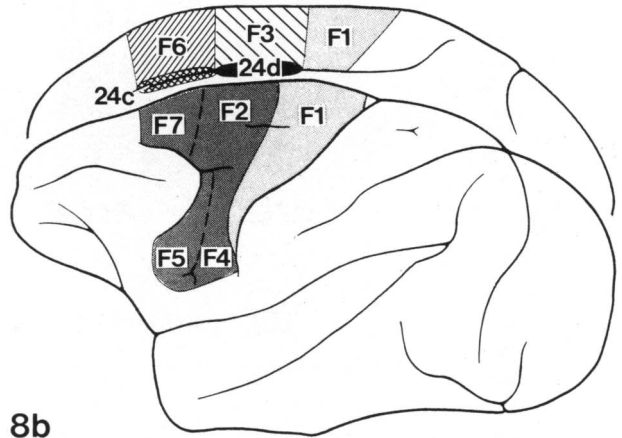
Fig. 7. Profile curves through the cortex of different sensorimotor areas and subareas in myelin-stained sections as quantitative descriptions of myeloarchitecture. For further explanation, see Figures 3–6. The laminar patterns of myelin densities of areas 4p, 4a and 6 (a) and areas 3a, 3b, 1 and 2 (7b) are shown.

shows a densely packed layer V, well demarcated from layers III and VI. All these features together lead to the impression of a clearly laminated area. No subdivisions of layer V can be observed and the overall cell density of F6 is less than in F3.

The laterodorsal and rostral parts of area 6 (area F7 of Matelli et al. 1991) have a prominent layer V, which is less dense than in F6. Layer VI is subdivided into 2



8a



8b

Fig. 8. Maps of the motor areas in the human (a) and macaque (b) cortex.

sublayers and lamination is clear. The rostral part of F7 has an incipient layer IV and shows no subdivision of layer V.

Area 24d (Fig. 2q) of Matelli et al. (1991), which could be the homologue of the human caudate cingulate motor area cmc according to its topology, has a thinner layer V than the rostrally adjacent 24c. Area 24c is the putative homologue of the human rostral cingulate motor area cmr. Area 24d shows a relatively clear-cut border between layers III/V. The

estimated as GLI (see Material and Methods) in each measuring field; this measure is given as relative density (GLI %), whereby the average density in a given cortical area is defined as 100%. The positions and extents of the cortical layers (Roman numerals) are indicated by bars in each figure. In order to make comparisons easier, the profile curves of two topographically adjoining areas are presented in the left figures, and the difference between these curves is shown to emphasise the differences in cytoarchitectural pattern between the areas (areas 4a and 6, Fig. 3a, b; areas 4a and 4p, Fig. 4a, b; areas 3b and 1, Fig. 5a, b; motor (areas 4p+4a+6) and somatosensory (areas 3a+3b+1) areas, Fig. 6a, b) in the right figures.



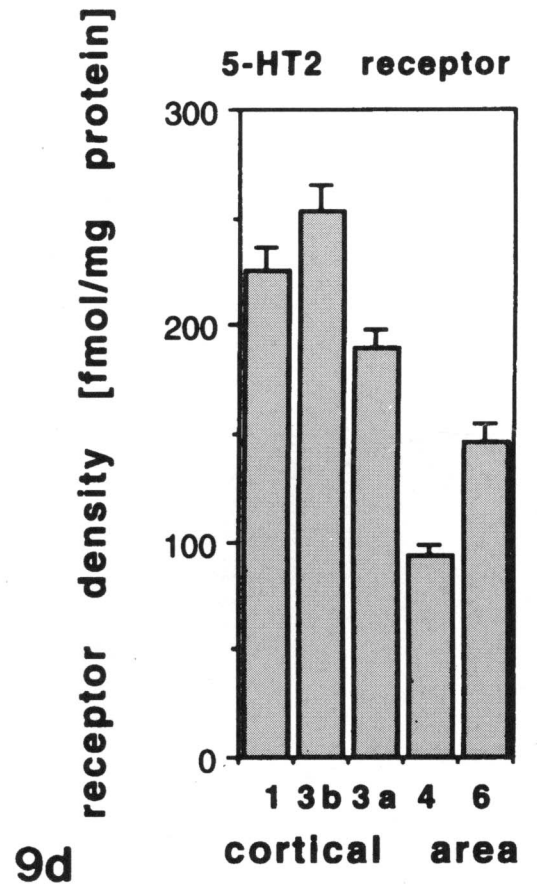
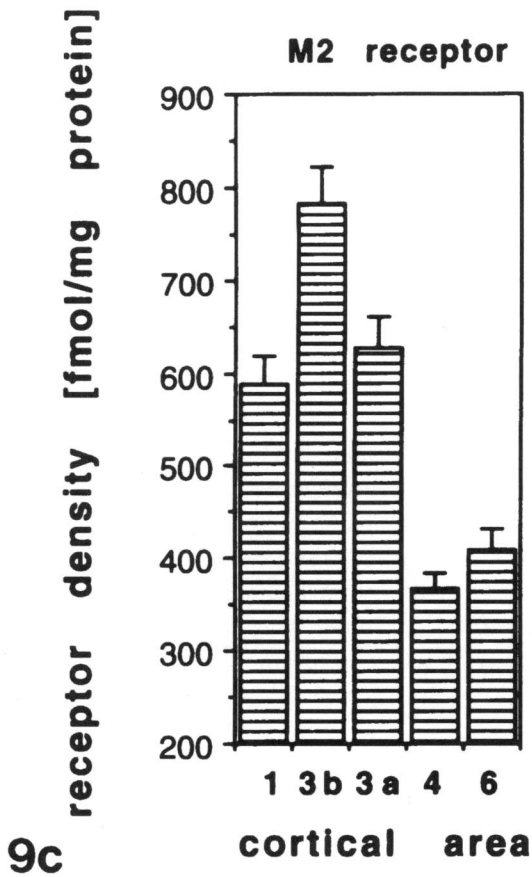
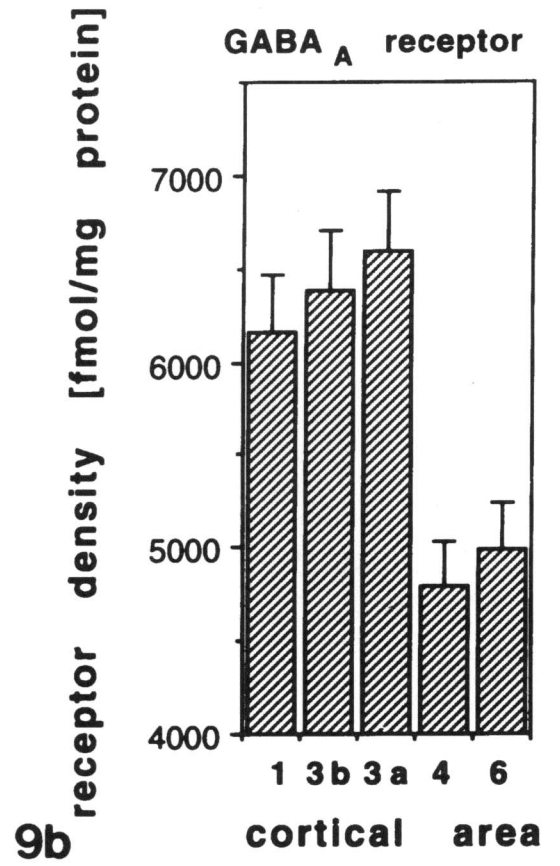
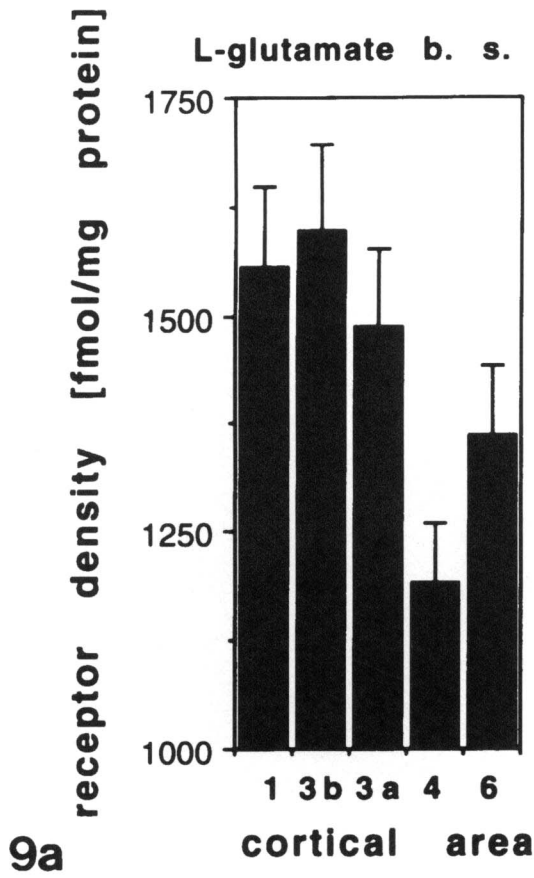


Fig. 9(a-d). For legend see opposite.

cells in layers III, VI and especially in layer V of 24d are larger than those in area 24c.

*Comparison of human and macaque sensorimotor cortices.* The cytoarchitecture and the topological relationships between the different areas of the human sensorimotor cortex show so many similarities to those of the macaque monkey that a common structural organisation can be assumed. In both species, areas 3b and 4 display practically identical cytoarchitectonic features. Only the overall cell packing density is higher in the macaque than the human cortex. This holds true not only for these two areas, but for the whole cortex. A minor difference between the two species seems to be the invasion of immediately adjacent parts of the neighbouring areas 3b and F3 (SMA-proper) by a few scattered giant pyramidal cells, which are restricted to area 4 in the human brain. The medium-sized to large pyramidal cells in areas F2 and F3 of the macaque are also found in the human SMA-proper (mesial part of area 6 $\alpha$  of Vogt & Vogt, 1919) and the caudal-laterodorsal premotor cortex (laterodorsal part of area 6 $\alpha$  of Vogt & Vogt, 1919). Whereas these cells are seen in a single row in the macaque cortex, they are more scattered in the human areas. Area 24d of the macaque has large pyramidal cells in layer V and precisely this is one of the characteristic features of the caudal cingulate motor area cmc1 in the human brain. The increase in the width of layer V from the human area cmc (macaque area 24d) to area cmr (macaque area 24c) is also common to both species. Furthermore, the clear demarcation of layers V and VI in the medially adjacent proisocortex of area 24b is an important cytoarchitectonic criterion for the separation of the proisocortical cingulate motor areas from the periallocortical cingulate area 24b in both species.

The mapping of the motor areas shows the same topological pattern in human and macaque brains (Fig. 8a–b). Area 4 (F1) is located in the central sulcus and on the precentral gyrus. The putative supplementary motor field is found on the mesial surface of the hemisphere and can be subdivided into caudal and rostral areas, which represent the SMA-proper (F3) and pre-SMA (F6), respectively. The dorsal parts of the premotor areas 6 $\alpha$  (F2) and 6 $\beta$  (F7) are located in a caudal-to-rostral sequence on the laterodorsal surface of the hemisphere. The areas cmc (24d) and cmr (24c) are bordered dorsally by the SMA-proper

and the pre-SMA, respectively. The mesial border of cmc and cmr is represented by the periallocortical anterior cingulate cortex (area 24b).

*Transmitter receptors in the different motor and somatosensory areas of the human and macaque brain*

*Human sensorimotor cortex.* The motor areas 4 and 6 can easily be separated from the somatosensory areas 3b and 1 and from the traditional area 3a on the basis of absolute receptor densities. The L-glutamate binding sites, GABA<sub>A</sub>, M2 and 5-HT<sub>2</sub> receptors show much higher densities in the somatosensory areas than in the motor areas (Fig. 9a–d). This difference in receptor densities is especially pronounced between the primary motor cortex and the primary somatosensory area 3b.

Within the group of frontal agranular motor fields all areas can be identified and separated from each other by differences in mean receptor densities. This has recently been demonstrated in detail (Zilles et al. 1995). Area 4 has the lowest mean densities of GABA<sub>A</sub>, muscarinic M1 and M2, kainate, 5-HT<sub>1</sub>,  $\alpha_1$  and  $\alpha_2$  receptors. The putative pre-SMA has higher densities of M2, NMDA,  $\alpha_1$  and 5-HT<sub>2</sub> receptors than the laterally adjoining premotor cortex (laterodorsal part of area 6 $\beta$ ). The inverse relationship between the receptor densities in both areas is found for AMPA and 5-HT<sub>1</sub> receptors. The density of M2 receptors is lower in cmr than in pre-SMA, but higher in the medially adjoining cingulate periallocortex; the NMDA, AMPA,  $\alpha_1$  and 5-HT<sub>2</sub> receptors, however, show higher densities in cmr than in pre-SMA. Fig. 10a–l shows examples of these quantitative data and of the patterns of laminar receptor distribution in colour coded autoradiographs.

The analysis of differences in laminar distribution patterns of receptors provides further evidence for the characterisation of the different motor areas. This approach corroborates and extends the parcellation based on cytoarchitectonic or myeloarchitectonic observations and on the measurements of mean receptor densities. Although most of the receptors show clear differences between their laminar patterns in the different motor and somatosensory areas, we will focus here, as an example, on the laminar patterns of 5-HT<sub>2</sub> receptors only. The motor areas 4 and 6 display the relatively highest densities in the more superficial layers I–III. Only area 4 reaches receptor

Fig. 9. Absolute densities (fmol/mg protein) of specific binding in different sensorimotor areas (areas 1, 3b, 3a, 4 and 6) of the human cortex. (a) shows the density of L-glutamate binding sites, (b) for GABA<sub>A</sub> receptors, (c) for muscarinic M2 receptors and (d) for serotonergic 5-HT<sub>2</sub> receptors.



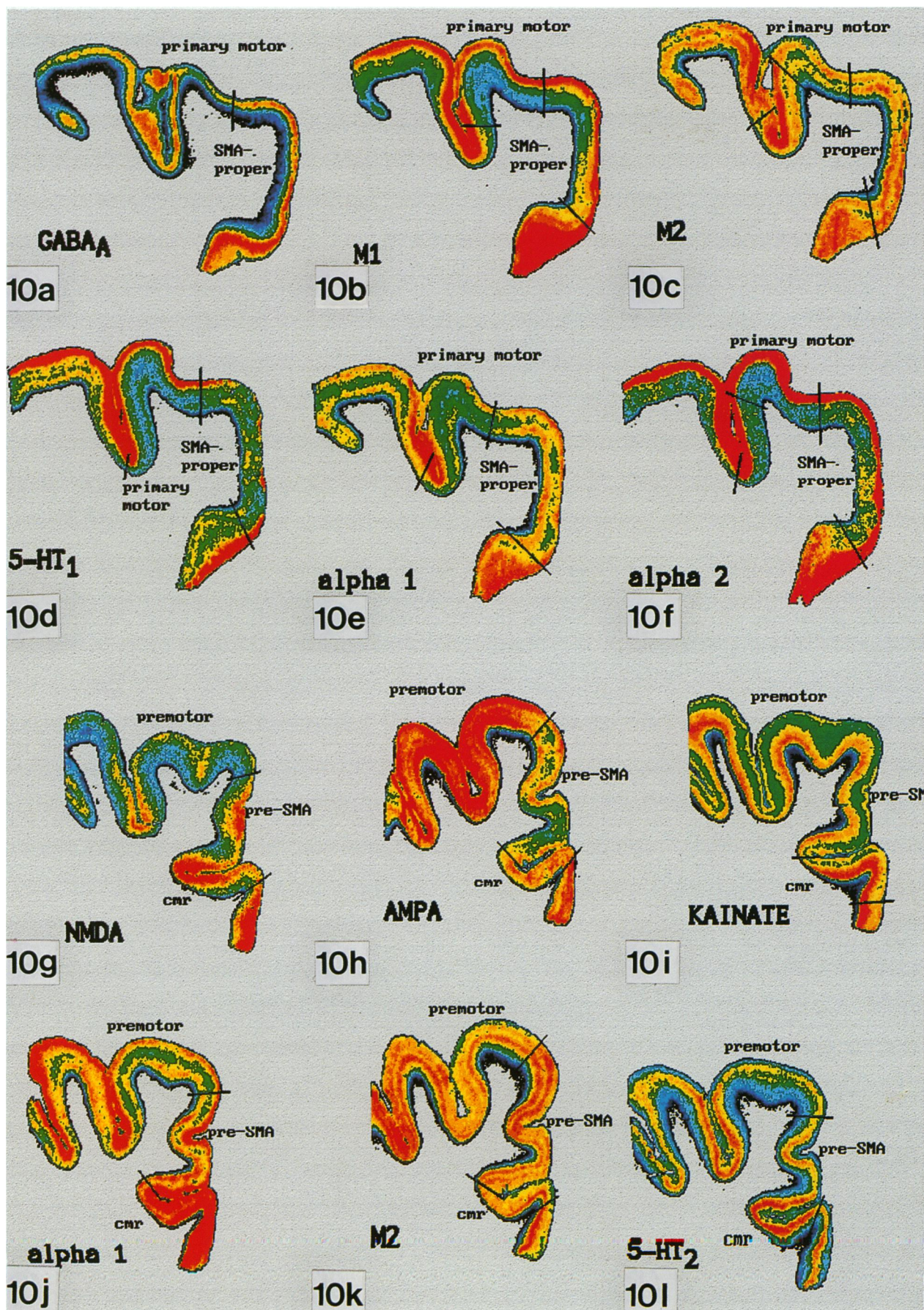
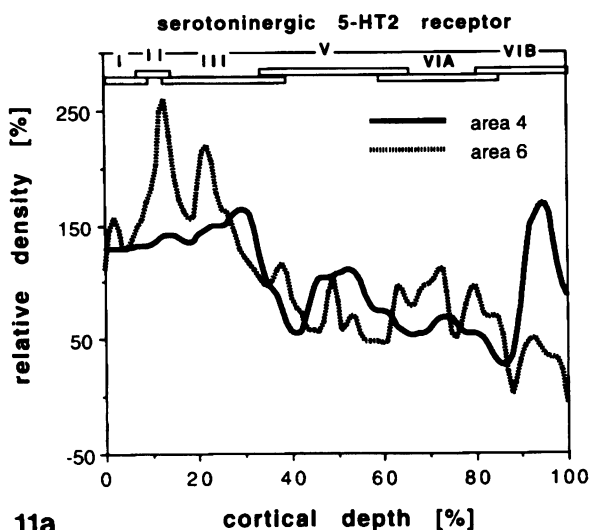
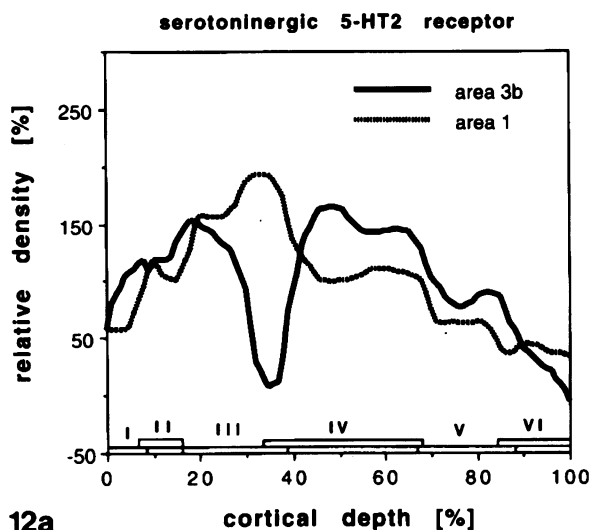


Fig. 10. For legend see opposite.

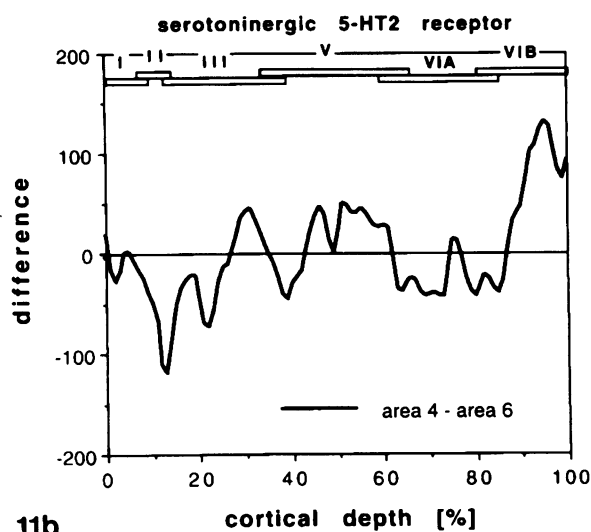




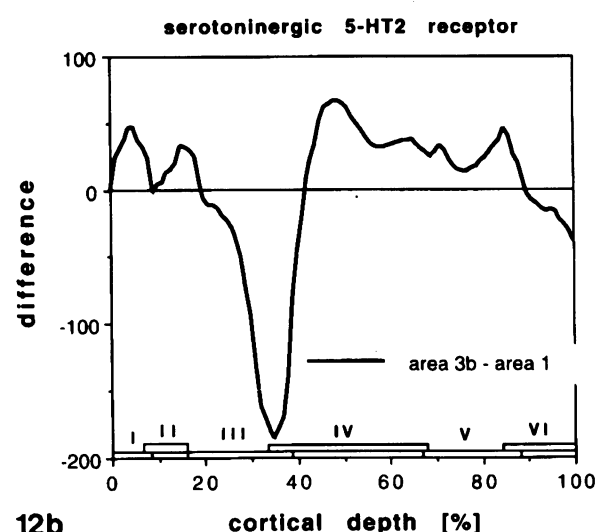
11a



12a



11b



12b

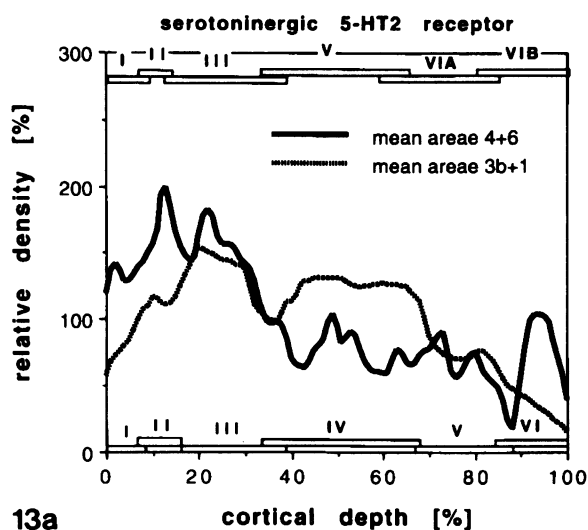
Fig. 11. Laminar distribution patterns of 5-HT<sub>2</sub> receptors in areas 4 and 6 of the human cortex (a). The total cortical thicknesses and receptor densities were transformed into relative scales (x-axis: total thickness of each area = 100%, pial surface = 0%, cortex/white matter border = 100%; y-axis: mean receptor density in each area = 100%). This transformation of data gives the clearest impression of interareal differences in laminar distribution patterns and allows direct comparison by excluding deformations of the profile curves caused by different absolute measures. (b) shows the difference between the two profile curves of (a). Places of greatest variations in relative receptor densities between areas can be precisely assigned to their relative location within the cortical depth.

densities above the mean value of 100% (Fig. 11a) in layer VIB. If the profile curve of the lateral area 6 (premotor cortex) is subtracted from that of area 4, the differences in laminar patterns between both motor areas are clearly visible (Fig. 11b). Area 6

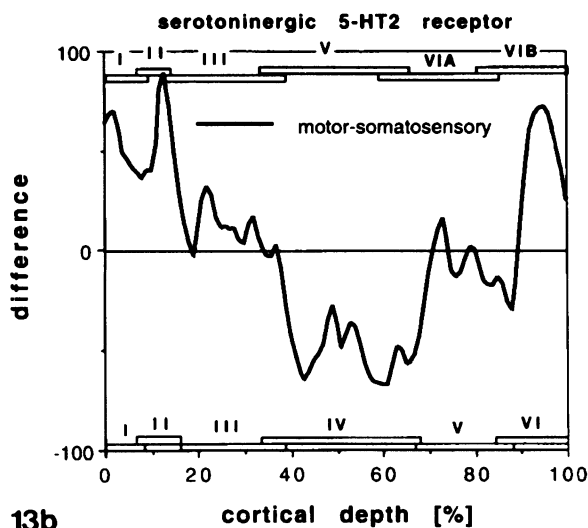
Fig. 12. Laminar distribution patterns of 5-HT<sub>2</sub> receptors in areas 3b and 1 of the human cortex (a) and the resulting difference curve (b). For further explanation, see Figure 11.

surpasses area 4 in receptor density in layers II, upper layer III and layer VIA, whereas area 4 surpasses area 6 in deeper layer III, layer V and VIB. The comparison of the laminar patterns of 5-HT<sub>2</sub> receptors between the somatosensory areas 3b and 1 also reveals clear-cut differences (Fig. 12a, b): area 3b surpasses area 1 in layers I–II and layer IV to upper layer VI, whereas the characteristic gap in lower layer III and upper layer IV seen in area 3b is colocalised with a peak in receptor density at this cortical depth in area 1. The comparison between motor areas (mean of areas 4 + 6) and somatosensory areas (mean of areas 3b + 1)

Fig. 10. Colour-coded autoradiographs of receptor distributions in motor areas of the human brain. The total binding of GABA<sub>A</sub> (a), muscarinic M1 (b) and M2 (c, k), serotonergic 5-HT<sub>1</sub> (d) and 5-HT<sub>2</sub> (l), noradrenergic  $\alpha_1$  (e, j) and  $\alpha_2$  (f) and glutamatergic NMDA (g), AMPA (h) and kainate (i) receptors is shown. Changes in receptor densities are found precisely at the borders between the architectonically defined areas.



13a



13b

Fig. 13. Laminar distribution patterns of 5-HT<sub>2</sub> receptors in motor (4+6) and somatosensory (3b+1) areas of the human cortex (a) and the resulting difference curve (b). For further explanation, see Figure 11.

demonstrates (Fig. 13a, b), that the motor areas have the higher receptor densities in layers I–III and VI, whereas the somatosensory areas reach higher values in layer IV. The relative receptor densities are approximately equal in layer V of both regions. In the same manner as shown here for the 5-HT<sub>2</sub> receptor all the other laminar distribution patterns of receptors were analysed.

Clear-cut differences were found between areas 3b and 1 in  $\alpha_1$  receptors and between areas 1, 3b, 4 and 6 in 5-HT<sub>1</sub> and M2 receptors. The other receptors (especially GABA<sub>A</sub> and M1) show only minor differences in laminar pattern between these areas. Kainate receptors are localised preferentially in the deeper layers of all motor areas. AMPA receptors show highest densities in a superficial and a deep

cortical band and NMDA receptors are found in the upper cortical layers.

*Macaque sensorimotor cortex.* Comparable differences between receptor densities as described above for the human sensorimotor areas can be found in the macaque brain. The somatosensory areas display higher absolute densities of L-glutamate binding sites, GABA<sub>A</sub> (Fig. 14b), M2 (Fig. 14a), kainate (Fig. 14c), 5-HT<sub>2</sub> and AMPA (Fig. 14d) receptors than the motor areas. The muscarinic M2 (Fig. 14a), serotonergic 5-HT<sub>2</sub> and glutamatergic AMPA (Fig. 14d) receptors show the most distinctive, i.e., the most heterogeneous distribution patterns in the lateral and mesial frontal agranular cortex. In most cases the cytoarchitectonic borders match precisely the places in which changes in density and laminar distribution pattern of these receptors occur. The term ‘laminar distribution pattern’ is used for the differential distribution of receptor densities over all layers of the cortex and not for the receptor densities in single layers; e.g. if the receptor densities are similar or identical in the upper cortical layers of two neighbouring areas, but different in the deeper layers a difference in the complex laminar pattern is reported. The border between areas 3a and F1 (area 4) is characterised by an abrupt decrease in GABA<sub>A</sub>, M2 and kainate receptors in the lower (M2, kainate) or upper (GABA<sub>A</sub>) layers of F1 (Fig. 14a–c). The borders between F1 and F2 (part of the premotor cortex) or F2 and F3 (SMA-proper) are marked by an increase in M2 (F1/F2) and AMPA (F2/F3) receptors in the deeper layers. The border between F3 and F6 (pre-SMA) is definable by further increases in M2 and AMPA receptors in F6 (not shown).

#### *Intersubject variability of human sensorimotor areas*

By comparing the localisation and extent of the primary motor area 4 and the primary somatosensory areas 1+2 in 3 human brains in the computerised brain atlas, a first impression of the intersubject variability of human sensorimotor areas can be gained (Fig. 15a–c). On the basis of cytoarchitectonic criteria the areal borders of areas 4, 3b, 1+2 together and 5 were identified first in histological sections and then transferred and delineated in MR images of the same brains. This procedure allows correction for histological artifacts (shrinkage, distortions during embedding, sectioning, mounting, etc.) on the basis of MR images taken during the life or post-mortem (Schormann et al. 1993, 1994), i.e. before histological procedures were begun. Afterwards, 3D reconstructions and surface rendering of each of these

brains were performed using the MR images with the labelled borders. Data on each of these brains can now be transformed to the format of the standard brain of a computerised brain atlas (Roland & Zilles, 1994). The resulting reconstructions are shown in Figure 15(a-c). Thus all structures of the 3 brains including the borders of cortical areas can be visualised and compared directly in the format of the standard brain of the atlas without being affected by differences in absolute brain size or overall brain shape. Only the intersubject variability in size and position of cortical areas contributes to the results. Figure 16 shows a first step towards a probability map of cortical areas by matching the single maps displayed in Figure 15(a-c). The darkest areas represent the places in which area 4 or areas 1+2 in all 3 brains coincide. These are the places, in which the respective cortical areas are located with highest probability in this small sample. The medium dark area indicates the places in which the respective cortical areas of only 2 brains coincide, and the light area where the cortical areas of only 1 of the 3 brains are encountered. Since the atlas database is open for any addition, this preliminary probability map will grow into a more representative map as the size of the sample increases.

Fig. 15d-f shows the results of a PET experiment with  $^{15}\text{O}$ -butanol as tracer. The subject was asked to execute simple movements of the index finger (Fig. 15d, e) or a sequential motor task (Fig. 15f). Details of the experiment are described in Schlaug et al. (1994) and Seitz & Roland (1992). The PET images (horizontal sections) represent data from a single subject and were coregistered with MR images from the same subject. This allows the macroscopic anatomical localisation of the brain regions active in the PET images. These images were then compared with the corresponding horizontal sections in the computerised brain atlas. Since the cytoarchitectonically defined areas are registered in the brain atlas, it is possible to compare the functional image with the cortical map in the atlas. The foci of activation in Figure 15d, e) coincide with area 4p of the primary motor cortex and area 3b of the primary somatosensory cortex contralateral to the active hand. Figure 15(f) shows the foci of activation in a sequential finger movement. The sequence was learned before the experiment. In addition to the previous areas, the supplementary motor cortex is active, in this case, on both sides of the brain. Figure 15(g, h) shows PET images ( $^{15}\text{O}$ -butanol as tracer) in the sagittal plane. In these cases the data of 10 subjects were averaged. The subjects were asked for tactile exploration of objects during PET recording (Fig.

15g) or to point, with eyes closed, to 7 randomly arranged targets after a cue (with open eyes) and delay period (Fig. 15h). The targets consisted of white spots on a blue background projected on a screen in front of the subjects. Details of both experiments are discussed in Kawashima et al. (1994) and Seitz et al. (1991). The first task involves mainly motor and somatosensory, the second task relies mainly on motor and visual modalities. The PET images were transferred to the computerised brain atlas. The activated brain regions in Fig. 15a are located in the motor areas 4p and 6 and in the somatosensory and parietal areas 1, 2 and 5. In Fig. 15h the activated areas match the cytoarchitectonically defined motor areas 4p and 6 and the parietal area 5.

## DISCUSSION

Since many invasive techniques (e.g. tracing of long fibre tracts, detailed electrophysiological mapping) applicable in animal experiments cannot be used in studies on the human brain, we rely on cyto-, myelo- and chemoarchitectonic approaches for a sufficiently detailed anatomical mapping of the human cortex. Comparisons between the cytoarchitecture of monkey and human brains are also important for detecting morphologically comparable areas for evaluating the nonhuman primate cortex as a model for the human cortex. Descriptive data collected on the human brain could then be evaluated by comparisons with experimental findings in the macaque.

Some differences in architectonic features of cortical areas were found between macaque and man. The cell density is generally higher in the monkey than in the human cortex. Betz cells as the extreme of a continuum of cell sizes were found to be restricted to area 4 in the human brain, but not distinctively so in the monkey cortex. The borders between many cortical areas seem to be more clearly recognisable in Nissl-stained sections or receptor autoradiographs of the human than of the macaque brain. Another example is the caudal cingulate motor area (area 24d in macaque brain), which shows large pyramidal cells in both species, but these cells reach nearly the size of giant pyramidal cells only in the human brain. All these observations argue for a more advanced differentiation and specialisation of isocortical areas in man than in the macaque. Despite these differences, the present findings also reveal great architectonic similarities between the sensorimotor cortices of both species. Above all, the topology of the sensorimotor areas is identical in both species. The distribution patterns of many receptors in the sensorimotor areas



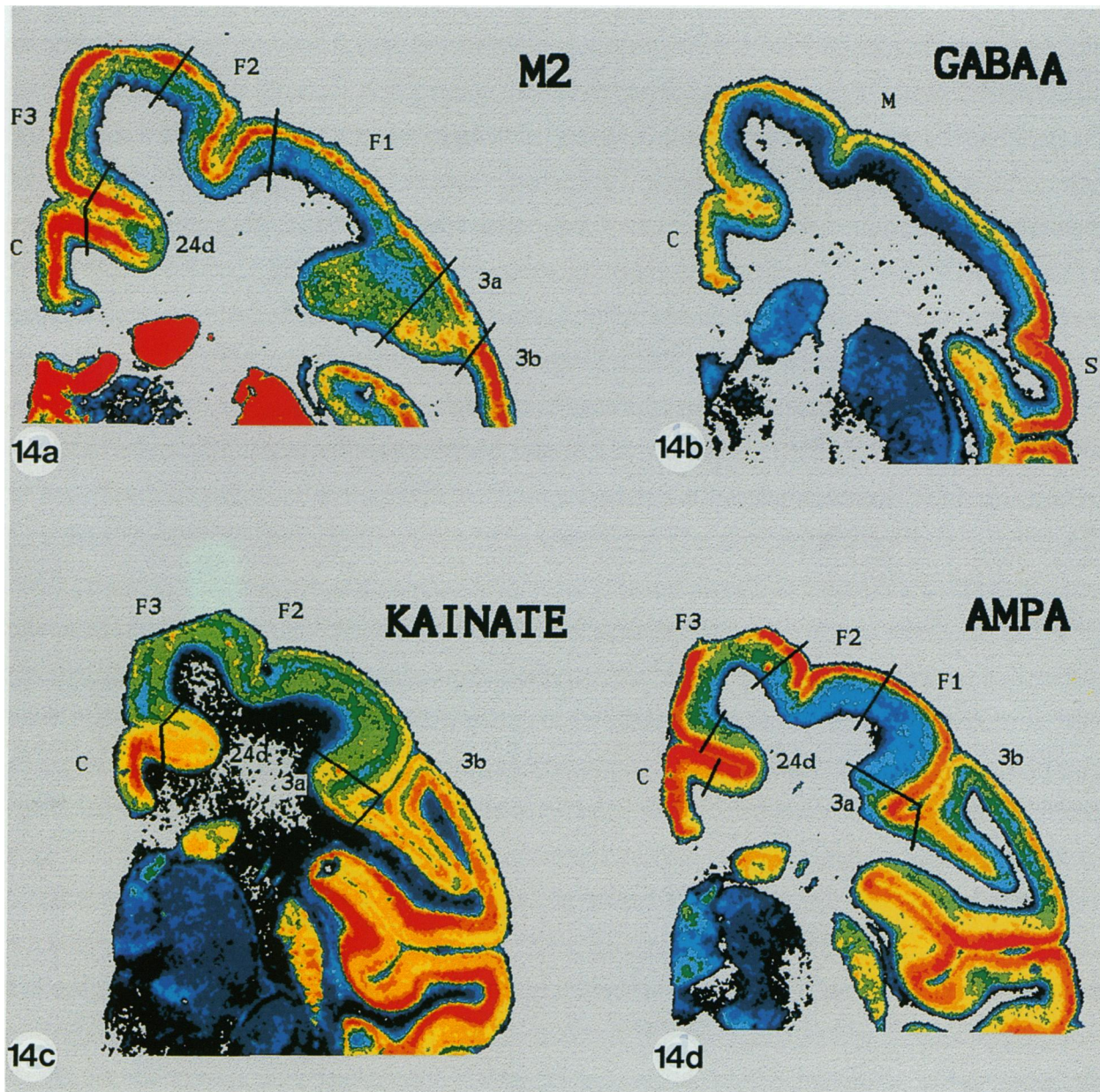


Fig. 14. Colour-coded autoradiographs of receptor distributions (*a*, muscarinic M2 receptor; *b*, GABA<sub>A</sub> receptor; *c*, glutamatergic kainate receptor; *d*, glutamatergic AMPA receptor) in sensorimotor areas of the macaque brain. Total binding is shown. M2, kainate and AMPA receptors show a more differentiated regional heterogeneity than GABA<sub>A</sub> receptors. Changes in receptor densities are found precisely at the borders between the architecturally defined areas. C, cingulate cortex; M, motor cortex; S, somatosensory cortex.

of both species also have many features in common. A sufficient interspecies comparability is therefore given, at least in the region of the sensorimotor cortex.

Although many receptor studies in the human cortex (e.g. Araujo et al. 1988; Biegon et al. 1986; Cowburn et al. 1988; Lin et al. 1986; Richards et al.

Fig. 15. Sensorimotor areas (areas 1 and 2 yellow; area 3b blue; area 4 red; area 5 green) in 3 human brains mapped by cytoarchitectonic and receptor autoradiographic criteria (*a-c*, left side) and transformed into the standard brain of the computerised brain atlas (*a-c*, right side). Areas 1, 2, 3b, 4p, 5, 6 and SMA are visible in PET images after activation in different motor and somatosensory tasks (*d-h*). In addition to the activation of areas 4 and 3b in a simple movement task, the supplementary motor cortex is revealed in a learned motor sequence task (*f*). The sagittal sections (*g-h*) are PET images after activation in tactile exploration and reaching tasks. The sections are 29 mm from the midline of the left hemisphere. (*g*) shows the average extent of activated areas in 10 subjects matching tactile shapes. By combining this image with the standard brain of the computerised brain atlas the activated areas can be identified as cytoarchitectonic areas 4p (part of the primary motor cortex), 1 and 2 (parts of the primary somatosensory cortex) and 5 (part of the posterior parietal cortex). (*h*) shows the average extent of activation in 10 subjects reaching out, with their eyes closed, to point to targets. By combining this image with the standard brain of the computerised brain atlas the activated areas can be identified as cytoarchitectonic areas 6, 4p and 5.



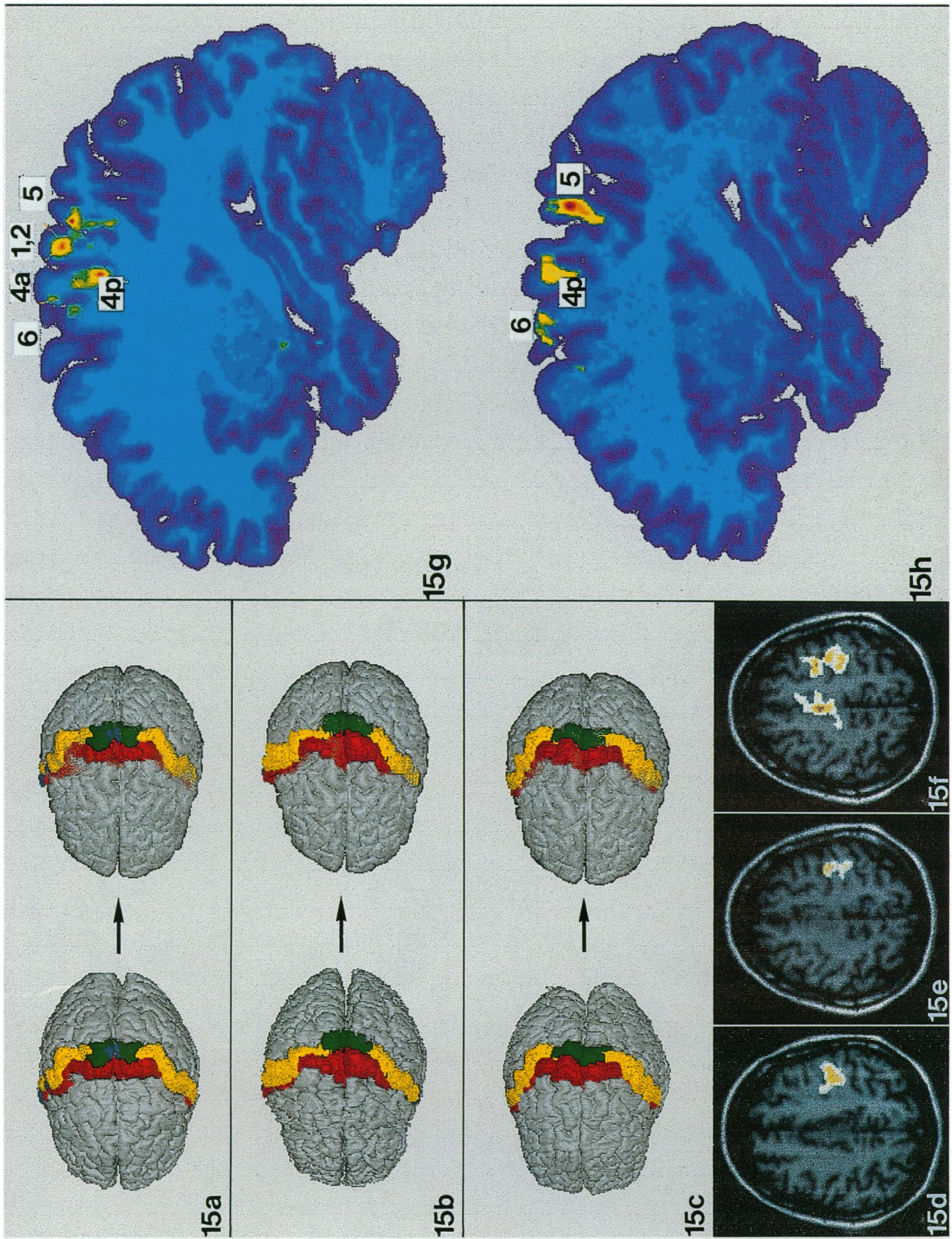


Fig. 15. For legend see opposite.



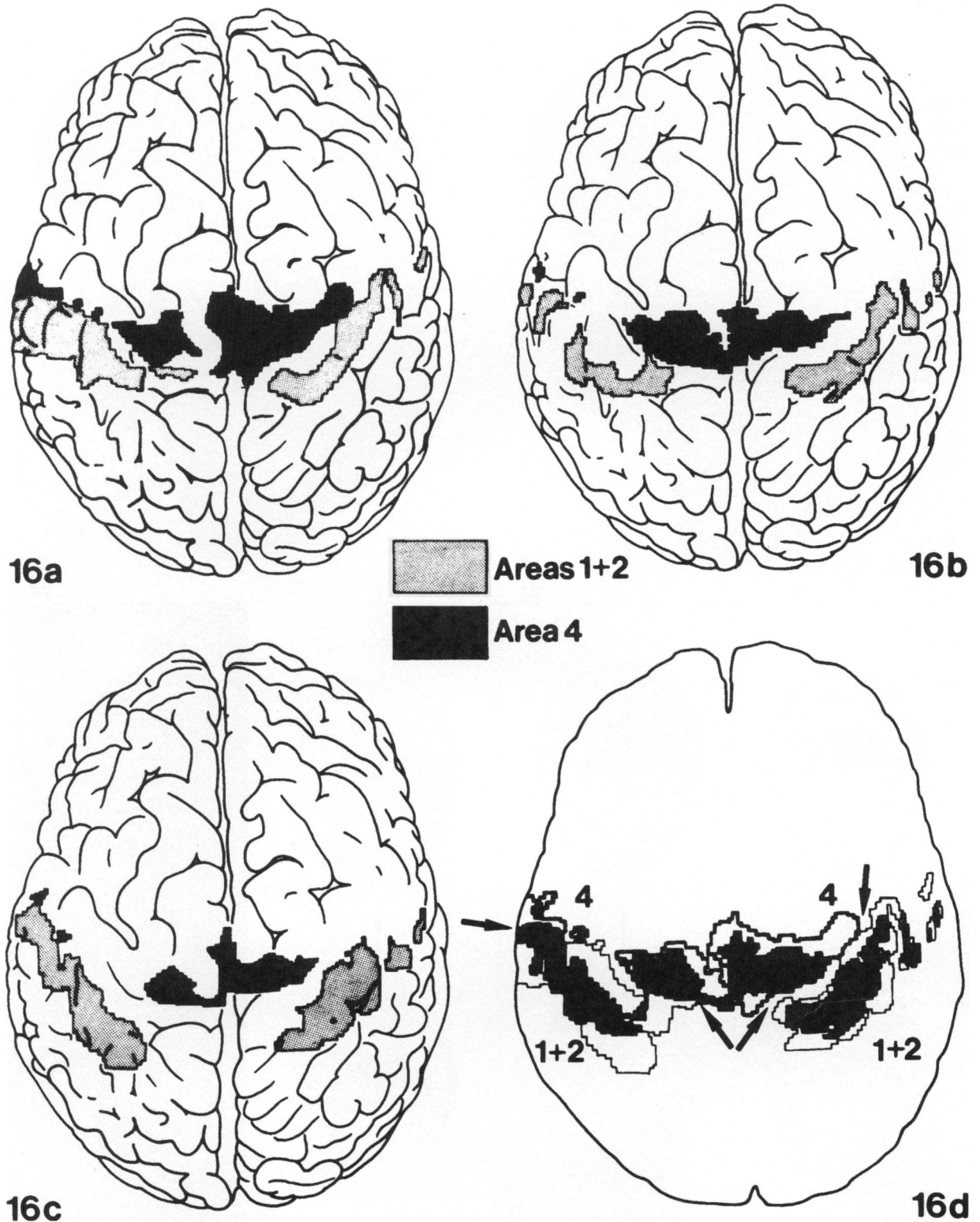


Fig. 16. Probability map of the localisation and extent of areas 4 and 1+2 in the human brain. (d) shows the representation of these areas on the dorsal surface of the standard brain after transfer from 3 individual brains (a-c) and adaptation to the standard brain of the atlas. Black indicates the extent to which the respective areas of all 3 brains are represented, grey and white indicate the extent to which only 2 or 1 brains, respectively, are found. The arrows in (d) mark the border between areas 4 and 1+2.

1987; Young & Chu, 1990) have enlarged our knowledge of its neurochemical aspects, almost none of these studies is based on a rigorous architectonic

analysis. Only rough anatomical identifications like 'frontal' or 'parietal' are given. In addition, some authors (Pazos et al. 1987a, b; Jansen et al. 1989,

1991; Gross-Isseroff et al. 1990*a, b*) have stated that all receptor binding sites, with the exception of those for 5-HT<sub>2</sub>, are more or less homogeneously distributed throughout the sensorimotor areas.

Our present and earlier studies (Zilles, 1991; Zilles & Schleicher, 1993; Zilles et al. 1993, 1995), however, show that many areal borders can be more clearly seen in the receptor autoradiographs than in cytoarchitectonic or myeloarchitectonic observations. This is only possible if receptor distribution is not homogeneous but heterogeneous. Obviously not all receptors are differentially distributed, but an approach using protocols for the simultaneous and quantitative demonstration of many different receptors in adjacent serial sections, as used in the present study, provides reliable data for cortical parcellation and evaluation of putative areal borders.

GABAergic cell bodies and synapses are most densely packed in layer II of the primary motor (Hendry et al. 1987) and in layers II and IV in the somatosensory areas of macaque monkeys (Hendry et al. 1987; Chudler et al. 1988). Immunohistochemistry of GABA<sub>A</sub> receptors revealed highest densities in layers II–IV and VI of an undefined area of the cerebral cortex (Richards et al. 1987). On autoradiography layer V contains 26% less GABA<sub>A</sub> receptors than layers II–III in an undefined area of the human isocortex (Young & Chu, 1990). Benzodiazepine receptors (Zezula et al. 1988) show the following density sequences in area 4 (II > VA > I > III > VB > VI) and areas 3, 1, 2 (III > IV > I + II > V > VI) of the human brain. The laminar distribution of GABA<sub>A</sub> receptors as visible in Figures 10 and 14 of the present report is therefore in accordance with the preferential localisation of presynaptic GABAergic structures in the more superficial part of the isocortex. GABA is important for the regulation of spatiotemporally organised ensembles of muscle activity in the primary motor cortex and to a lesser degree in the premotor cortex (Matsumara et al. 1991). The receptive field size of rapidly adapting neurons in the primary somatosensory cortex is defined by GABAergic inhibition. Loss or restriction of this inhibitory mechanism leads to an increase in receptive field size (Alloway & Burton, 1991). This difference between GABAergic function in motor versus somatosensory regions is paralleled by a quantifiable difference in GABA<sub>A</sub> receptor densities between both regions with a generally higher density in the somatosensory areas.

Choline acetyltransferase (ChAT) activity does not differ significantly between human frontal and parietal cortices (Araujo et al. 1988). However, the density of

muscarinic M1 and M2 receptors does differ between both regions with 84% and 29% higher densities in the frontal cortex (Araujo et al. 1988). Other data (Lin et al. 1986), however, do not corroborate this regional difference for M1 receptors. For the first time we have seen a regional inhomogeneity of muscarinic M1 and M2 receptors not only between somatosensory and motor regions, but also between the different motor areas. Especially the M2 receptor densities and laminar patterns differ significantly between cytoarchitectonically defined areas. Probably the transmitter-mediated effects of the regionally homogeneously distributed cholinergic axons are differentiated by the inhomogeneously distributed receptors.

L-glutamate binding sites show a similar mean density in frontal and parietal human cortices (Cowburn et al. 1988). However, Jansen et al. (1989) reported on a 57% lower density of such sites in the somatosensory than in the motor cortex; the laminar pattern in the motor cortex is I + II + III ≥ V + VI and in the somatosensory cortex V + VI > I + II + III. Here we have presented for the first time data defining the regionally inhomogeneous distributions of NMDA, AMPA and kainate receptors in the human and macaque sensorimotor areas. The differential laminar distribution of NMDA and non-NMDA receptors and the regional heterogeneity of these receptors are apparently functionally important because recent data (Shima & Tanji, 1993) have shown that NMDA and glutamatergic non-NMDA receptors are differentially involved in motor task-related neuronal activity in the various agranular motor areas of macaques. The blockade of NMDA receptors preferentially suppressed spontaneous discharge, whereas the blockade of non-NMDA receptors suppressed more selectively movement-related functions. The suppression of both classes of glutamate receptors affected set-related neuronal activities.

The precentral and postcentral gyri belong to those regions in the human cortex with the highest serotonin levels (Herregodts et al. 1991). Serotonin-immunoreactive fibres are the most densely packed in layer I followed by layers II to upper III, very low in deeper III and IV and moderate in layers V and VI in the macaque primary somatosensory cortex (DeFelipe & Jones 1988); in the motor cortex layers V and VI show a low density. Serotonin (5-HT)-containing varicosities are more frequent in the somatosensory than in the motor and premotor areas of the macaque. The varicosities are evenly distributed throughout the cortical layers with the exception of a low density in

deep layer III of area 4 (Berger et al. 1988). Biegon et al. (1986), Gross-Isseroff et al. (1990b) and Pazos et al. (1987*a, b*) reported a fairly homogeneous regional distribution of 5-HT<sub>1</sub> and 5-HT<sub>2</sub> receptors throughout the human cortex. The present data, however, clearly showed that 5-HT<sub>1</sub> and 5-HT<sub>2</sub> receptor densities are not evenly distributed. These discrepancies may be reconciled by the fact that different techniques were used and receptor data was not correlated with cytoarchitectonically defined parcellations in the earlier studies. Many of the regional differences in receptor densities are visible only after contrast enhancement with an image analyser, and measurements of densities are only reliable in an architectonic context if the cortical area is defined by correlated cytoarchitectonics. The description of macroscopic features such as gyri and sulci does not seem to be sufficient for the analysis of areal inhomogeneities. 5-HT<sub>1</sub> receptors show the highest densities in layers I–II of area 4 and much lower densities in the deeper layers (Pazos et al. 1987*b*). 5-HT<sub>2</sub> receptors in the precentral and postcentral gyri show the highest concentrations in the middle and much lower concentrations in the other layers (Gross-Isseroff et al. 1990*b*; Pazos et al. 1987*b*). These findings are corroborated by the present data.

The highest densities of noradrenaline-containing nerve fibres occur in the human primary motor and somatosensory cortices (Gaspar et al. 1989) with a slight preponderance in layers III and V. The adjoining premotor and parietal association areas display lower densities when compared with the precentral and postcentral gyri.  $\alpha_1$ -Adrenoceptors are slightly more concentrated in the postcentral than in the precentral gyrus (Gross-Isseroff et al. 1990*a*); in both regions they are much more densely packed in the outer third of the cortex than in the inner two thirds. The present data corroborate and extend these findings in the human sensorimotor cortex.

The mesial part of the macaque area 6 contains the supplementary motor field, which can be subdivided into at least a caudal (SMA-proper) and a rostral part (pre-SMA) (Tanji et al. 1980; Macpherson et al. 1982; Wiesendanger & Wiesendanger, 1985; Mitz & Wise, 1987; Luppino et al. 1990, 1991, 1993; Mushiake et al. 1990; Matelli et al. 1991; Matsuzaka et al. 1993). The lateral part of area 6 represents the premotor cortex, which has also been subdivided into several areas (Vogt & Vogt, 1919, 1926; Muakkassa & Strick, 1979; Sessle & Wiesendanger, 1982; Wise & Strick, 1984; Fries, 1985; Matelli et al. 1985, 1986, 1989, 1991; Wise, 1985*a, b*; Barbas & Pandya, 1987; Okano & Tanji, 1987; Wise & Godschalk, 1987; Strick, 1988;

Tanji & Kurata, 1989; Rizzolatti et al. 1990; Dum & Strick, 1991; He et al. 1993). In addition, two motor areas in the upper part of the anterior cingulate cortex have been described in the monkey (Luppino et al. 1991; Matelli et al. 1991) as areas 24d and 24c. The present cytoarchitectonic results on the macaque cortex are in agreement with these reports, especially with the observations of Matelli et al. (1985, 1986, 1989, 1991) and Luppino et al. (1990, 1991, 1993), and the receptor autoradiographic data show the same locations of borders as defined in the correlative cytoarchitectonic delineations on neighbouring Nissl-stained sections.

The evidence for parcellation of the human sensorimotor cortex comes mainly from architectonic studies, observations of patients with lesions and PET imaging (Brodmann, 1903, 1905/06, 1909; Vogt, 1910; Economo & Koskinas, 1925; Fulton, 1935; Penfield & Welch, 1949, 1951; Sarkissov et al. 1955; Sanides, 1962, 1964; Braak, 1976, 1979, 1980; Roland et al. 1980*a, b*, 1982; Mazziotta et al. 1985; Freund, 1987, 1991; Halsband & Freund, 1990; Seitz et al. 1990; Colebatch et al. 1991; Deiber et al. 1991; Fried et al. 1991; Frith et al., 1991; Grafton et al. 1992; Kurata, 1992; Seitz & Roland, 1992; Matelli et al. 1993; Paus et al. 1993; Roland, 1993; Kawashima et al. 1994; Schlaug et al. 1994). The cytoarchitectonic maps of some of these authors, however, do not present a sufficiently consistent pattern and neither can they be directly integrated with recent PET studies. This is because they are highly schematic and not representative (evidence from only one or a few brains; data summarised in schematic drawings) and because the authors lacked tools for integrating images from different modalities. By contrast, the present quantitative cytoarchitectonic analysis of the human primary somatosensory motor, SMA-proper, pre-SMA, cingulate motor areas and the dorsolateral part of area 6 can be integrated with receptor distributions by alternatingly processed sections and with PET data on the basis of a recently developed computerised brain atlas and software for integrating data from MR images and histological sections (Schormann et al. 1993, 1994; Roland et al. 1994; Roland & Zilles, 1994). This results in good agreement between the data from different modalities. Moreover, the computerised brain atlas is a system open to new spatially definable observations (Roland & Zilles, 1994), which allows the permanent integration of additional data and thus the creation of a database with increasing representativity.



## ACKNOWLEDGEMENTS

This work was supported by grants from the DFG (SFB 194/A6), HSFP, HCMP and ENP. Thanks are due to Kristina Rascher for improving the linguistic style.

## REFERENCES

- ALLOWAY KD, BURTON H (1991) Differential effects of GABA and bicuculline on rapidly- and slowly-adapting neurons in primary somatosensory cortex of primates. *Experimental Brain Research* **85**, 598–610.
- ARAUJO DM, LAPCHAK PA, ROBITAILLE Y, GAUTHIER S, QUIRION R (1988) Differential alteration of various cholinergic markers in cortical and subcortical regions of human brain in Alzheimer's disease. *Journal of Neurochemistry* **50**, 1914–1923.
- BARBAS, H., PANDYA DN (1987) Architecture and frontal cortical connections of the premotor cortex (area 6) in the rhesus monkey. *Journal of Comparative Neurology* **256**, 211–228.
- BERGER B, TROTTIER S, VERNEY C, GASPAR P, ALVAREZ C (1988) Regional and laminar distribution of the dopamine and serotonin innervation in the macaque cerebral cortex: a radioautographic study. *Journal of Comparative Neurology* **273**, 99–119.
- BIEGON A, KARGMAN S, SNYDER L, MCEWEN BS (1986) Characterization and localization of serotonin receptors in human brain postmortem. *Brain Research* **363**, 91–98.
- BRAAK H (1976) A primitive gigantopyramidal field buried in the depth of the cingulate sulcus of the human brain. *Brain Research* **109**, 219–223.
- BRAAK H (1979) The pigment architecture of the human frontal lobe. I. Precentral, subcentral and frontal region. *Anatomy and Embryology* **157**, 35–68.
- BRAAK H (1980) *Architectonics of the Human Telencephalic Cortex*. Berlin, New York: Springer.
- BRODMANN K (1903) Beiträge zur histologischen Lokalisation der Grosshirnrinde. Erste Mitteilung: Die Regio Rolandica. *Journal für Psychologie und Neurologie* **2**, 79–107.
- BRODMANN K (1905/06) Beiträge zur histologischen Lokalisation der Grosshirnrinde. V. Mitteilung. Über den allgemeinen Bau des Cortex pallii bei den Mammaliern und zwei homologe Rindenfelder im besonderen. Zugleich ein Beitrag zur Furchenlehre. *Journal für Psychologie und Neurologie* **6**, 275–400.
- BRODMANN K (1909) *Vergleichende Lokalisationslehre der Grosshirnrinde in ihren Prinzipien dargestellt auf Grund des Zellenbaues*. Leipzig: Barth.
- CAMPBELL AW (1905) *Historical Studies on the Localization of Cerebral Function*. Cambridge: Cambridge University Press.
- CHUDLER EH, PRETEL S, KENSHALO DR (1988) Distribution of GAD-immunoreactive neurons in the first (SI) and second (SII) somatosensory cortex of the monkey. *Brain Research* **456**, 57–63.
- COLEBATCH JG, DEIBER M-P, PASSINGHAM RE, FRISTON J, FRACKOWIAK RSJ (1991) Regional cerebral blood flow during voluntary arm and hand movements in human subjects. *Journal of Neurophysiology* **65**, 1392–1401.
- COWBURN R, HARDY J, ROBERTS P, BRIGGS R (1988) Regional distribution of pre- and postsynaptic glutamatergic function in Alzheimer's disease. *Brain Research* **452**, 403–407.
- DEFELIPE J, JONES EG (1988) A light and electron microscopic study of serotonin-immunoreactive fibers and terminals in the monkey sensory-motor cortex. *Experimental Brain Research* **71**, 171–182.
- DEIBER MP, PASSINGHAM RE, COLEBATCH JG, FRISTON KJ, NIXON PD, FRACKOWIAK RSJ (1991) Cortical areas and the selection of movement: a study with positron emission tomography. *Experimental Brain Research* **84**, 393–402.
- DUM RP, STRICK PL (1991) The origin of corticospinal projections from the premotor areas in the frontal lobe. *Journal of Neuroscience* **11**, 667–689.
- ECONOMO C VON, KOSKINAS GN (1925) *Die Cytoarchitektonik der Hirnrinde des erwachsenen Menschen*. Berlin: Springer.
- FERRIER D (1886) *The Functions of the Brain*. New York: G. P. Putnam.
- FOERSTER O (1936) Motorische Felder und Bahnen. In *Handbuch der Neurologie*, vol. 6 (ed. O. Bumke & O. Foerster), pp. 1–357. Berlin: Springer.
- FREUND H-J (1987) Abnormalities of motor behaviour after cortical lesions in man. In *Handbook of Physiology*, section 1: *The Nervous System*, vol. V: *Higher Functions of the Brain*, part 2 (section ed. V. B. Mountcastle, vol. ed. F. Plum), pp. 763–810. Baltimore: Williams and Wilkins.
- FREUND H-J (1991) What is the evidence for multiple motor areas in the human brain? In *Motor Control: Concepts and Issues* (ed. D. R. Humphrey & H.-J. Freund), pp. 399–411. Chichester: John Wiley & Sons.
- FRIED I, KATZ A, MCCARTHY G, SASS KJ, WILLIAMSON P, SPENCER SS, SPENCER DD (1991) Functional organization of human supplementary motor cortex studied by electrical stimulation. *Journal of Neuroscience* **11**, 3656–3666.
- FRIES W (1985) Inputs from motor and premotor cortex to the superior colliculus of the macaque monkey. *Behavioural Brain Research* **18**, 95–105.
- FRITH CD, FRISTON K, LIDDLE PF, FRACKOWIAK RSJ (1991) Willed action and the prefrontal cortex in man: a study with PET. *Proceedings of the Royal Society of London, Series B, Biological Sciences* **244**, 241–246.
- FRITSCH GT, HITZIG JE (1870) Über die elektrische Erregbarkeit des Grosshirns. *Archiv für Anatomie, Physiologie und wissenschaftliche Medizin* **37**, 300–332.
- FULTON JF (1935) Definition of the motor and premotor areas. *Brain Research* **58**, 311–316.
- GASPAR P, BERGER B, FEBVRET A, VIGNY A, HENRY JP (1989) Catecholamine innervation of the human cerebral cortex as revealed by comparative immunohistochemistry of tyrosine hydroxylase and dopamine-beta-hydroxylase. *Journal of Comparative Neurology* **279**, 249–271.
- GRAFTON ST, MAZZIOTTA JC, PRESTY S, FRISTON KJ, FRACKOWIAK RSJ, PHELPS ME (1992) Functional anatomy of human procedural learning determined with regional cerebral blood flow and PET. *Journal of Neuroscience* **12**, 2542–2548.
- GROSS-ISSEROFF R, DILLON KA, FIELDUST SJ, BIEGON A (1990a) Autoradiographic analysis of  $\alpha_1$ -noradrenergic receptors in the human brain postmortem. *Archives of General Psychiatry* **47**, 1049–1053.
- GROSS-ISSEROFF R, SALAMA D, ISRAELI M, BIEGON A (1990b) Autoradiographic analysis of age-dependent changes in serotonin 5-HT<sub>2</sub> receptors of the human brain postmortem. *Brain Research* **519**, 223–227.
- GRÜNBAUM ASF, SHERRINGTON CS (1903) Observations on the physiology of the cerebral cortex in anthropoid apes. *Proceedings of the Royal Society of London, Series B, Biological Sciences* **72**, 152–155.
- HALSBAND U, FREUND H-J (1990) Premotor cortex and conditional motor learning in man. *Brain* **113**, 207–222.
- HE S-Q, DUM RP, STRICK PL (1993) Topographic organization of corticospinal projections from the frontal lobe: motor areas on the lateral surface of the hemisphere. *Journal of Neuroscience* **13**, 952–980.
- HENDRY SHC, SCHWARK HD, JONES EG, YAN J (1987) Numbers and proportions of GABA-immunoreactive neurons in different areas of monkey cerebral cortex. *Journal of Neuroscience* **7**, 1503–1519.
- HERREGODTS P, EBINGER G, MICHOTTE Y (1991) Distribution of monoamines in human brain: evidence for neurochemical

- heterogeneity in subcortical as well as in cortical areas. *Brain Research* **542**, 300–306.
- JACKSON JH (1863) Convulsive spasms of the right hand and arm preceding epileptic seizures. *Medical Times and Gazette* **1**, 589.
- JACKSON JH (1870) A study of convulsions. *Transactions of the St Andrew's Medical Graduates Association* **3**, 162–204.
- JANSEN KLR, FAULL RLM, DRAGUNOW M (1989) Excitatory amino acid receptors in the human cerebral cortex: a quantitative autoradiographic study comparing the distributions of [<sup>3</sup>H]TCP, [<sup>3</sup>H]glycine, L-[<sup>3</sup>H]glutamate, [<sup>3</sup>H]AMPA and [<sup>3</sup>H]kainic acid binding sites. *Neuroscience* **32**, 587–607.
- JANSEN KLR, FAULL RLM, DRAGUNOW M, LESLIE RA (1991) Distribution of excitatory and inhibitory amino acid, sigma, monoamine, catecholamine, acetylcholine, opioid, neurotensin, substance P, adenosine and neuropeptide Y receptors in human motor and somatosensory cortex. *Brain Research* **566**, 225–238.
- JONES EG, PORTER R (1980) What is area 3a? *Brain Research Reviews* **2**, 1–43.
- KAWASHIMA R, ROLAND PE, O'SULLIVAN BT (1994) Fields in human motor areas involved in preparation for reaching, actual reaching, and visuomotor learning: a positron emission tomography study. *Journal of Neuroscience* **14**, 3462–3474.
- KRAUSE F (1911) *Chirurgie des Gehirns und Rückenmarks nach eigenen Erfahrungen*. Berlin: Urban and Schwarzenberg.
- KURATA K (1992) Somatotopy in the human supplementary motor area. *Trends in Neuroscience* **15**, 159–160.
- LEMON R (1988) The output map of the primate motor cortex. *Trends in Neuroscience* **11**, 501–506.
- LIN S-C, OLSON KC, OKAZAKI H, RICHELSON E (1986) Studies on muscarinic binding sites in human brain identified with [<sup>3</sup>H]pirenzepine. *Journal of Neurochemistry* **46**, 274–279.
- LUPPINO G, MATELLI M, RIZZOLATTI G (1990) Cortico-cortical connections of two electrophysiologically identified arm representations in the mesial agranular frontal cortex. *Experimental Brain Research* **82**, 214–218.
- LUPPINO G, MATELLI M, CAMARDA RM, GALLESE V, RIZZOLATTI G (1991) Multiple representations of body movements in mesial area 6 and the adjacent cingulate cortex: an intracortical microstimulation study in the macaque monkey. *Journal of Comparative Neurology* **311**, 463–482.
- LUPPINO G, MATELLI M, CAMARDA R, RIZZOLATTI G (1993) Corticocortical connections of area F3 (SMA-Proper) and area F6 (pre-SMA) in the macaque monkey. *Journal of Comparative Neurology* **338**, 114–140.
- MACPHERSON JM, MARANGOZ C, MILES TS, WIESENDANGER M (1982) Microstimulation of the supplementary motor area (SMA) in the awake monkey. *Experimental Brain Research* **45**, 410–416.
- MATELLI M, LUPPINO G, RIZZOLATTI G (1985) Patterns of cytochrome oxidase activity in the frontal agranular cortex of the macaque monkey. *Behavioural Brain Research* **18**, 125–137.
- MATELLI M, CAMARDA R, GLICKSTEIN M, RIZZOLATTI G (1986) Afferent and efferent projections of the inferior area 6 in the macaque monkey. *Journal of Comparative Neurology* **251**, 281–298.
- MATELLI M, LUPPINO G, FOGASSI L, RIZZOLATTI G (1989) Thalamic input to inferior area 6 and area 4 in the macaque monkey. *Journal of Comparative Neurology* **280**, 458–488.
- MATELLI M, LUPPINO G, RIZZOLATTI G (1991) Architecture of superior and mesial area 6 and adjacent cingulate cortex in the macaque monkey. *Journal of Comparative Neurology* **311**, 445–462.
- MATELLI M, RIZZOLATTI G, BETTINARDI V, GILARDI MC, PERANI D, RIZZO G et al. (1993) Activation of precentral and mesial motor areas during the execution of elementary proximal and distal arm movements: a PET study. *NeuroReport* **4**, 1295–1298.
- MATSUMARA M, SAWAGUCHI T, OISHI T, UEKI K, KUBOTA K (1991) Behavioral deficits induced by local injection of bicuculline and muscimol into the primate motor and premotor cortex. *Journal of Neurophysiology* **65**, 1542–1553.
- MATSUZAKA Y, AIZAWA H, TANJI J (1993) A motor area rostral to the supplementary motor area (presupplementary motor area) in the monkey: neuronal activity during a learned motor task. *Journal of Neurophysiology* **68**, 653–662.
- MAZZIOTTA JC, PHELPS ME, WAPENSKI J (1985) Human cerebral motor system metabolic responses in health and disease. *Journal of Cerebral Blood Flow and Metabolism* **5**, 213–214.
- MITZ AR, WISE SP (1987) The somatotopic organization of the supplementary motor area: intracortical microstimulation mapping. *Journal of Neuroscience* **7**, 1010–1021.
- MUAKKASSA KF, STRICK PL (1979) Frontal lobe inputs to primate motor cortex: evidence for four somatotopically organized 'premotor' areas. *Brain Research* **177**, 176–182.
- MUSHIAKE H, INASE M, TANJI J (1990) Selective coding of motor sequence in the supplementary motor area of the monkey cerebral cortex. *Experimental Brain Research* **82**, 208–210.
- OKANO K, TANJI J (1987) Neuronal activity in the primate motor fields of the agranular frontal cortex preceding visually triggered and self-paced movements. *Experimental Brain Research* **66**, 155–166.
- PAUS T, PETRIDES M, EVANS AC, MEYER E (1993) Role of the human anterior cingulate cortex in the control of oculomotor, manual and speech responses: a positron emission tomography study. *Journal of Neurophysiology* **70**, 453–469.
- PAZOS A, PROBST A, PALACIOS JM (1987a) Serotonin receptors in the human brain. III. Autoradiographic mapping of serotonin-1 receptors. *Neuroscience* **21**, 97–122.
- PAZOS A, PROBST A, PALACIOS JM (1987b) Serotonin receptors in the human brain. IV. Autoradiographic mapping of serotonin-2 receptors. *Neuroscience* **21**, 123–139.
- PENFIELD W, RASMUSSEN T (1950) *The Cerebral Cortex of Man*. New York: Macmillan.
- PENFIELD W, WELCH K (1949) The supplementary motor area in the cerebral cortex of man. *Transactions of the American Neurological Association* **74**, 179–184.
- PENFIELD W, WELCH K (1951) The supplementary motor area of the cerebral cortex. *Archives of Neurology and Psychiatry* **66**, 289–317.
- RICHARDS JG, SCHOCH P, HÄRING P, TAKACS B, MÖHLER H (1987) Resolving GABA<sub>A</sub>/benzodiazepine receptors: cellular and subcellular localization in the CNS with monoclonal antibodies. *Journal of Neuroscience* **7**, 1866–1886.
- RIZZOLATTI G, GENTILUCCI M, CAMARDA V, GALLESE G, LUPPINO G, MATELLI M (1990) Neurons related to reaching-grasping arm movements in the rostral part of area 6 (area 6aβ). *Experimental Brain Research* **82**, 337–350.
- ROLAND PE (1993) *Brain Activation*. New York: John Wiley & Sons.
- ROLAND PE, ZILLES K (1994) Brain atlases – A new research tool. *Trends in Neuroscience* **17**, 458–467.
- ROLAND PE, LARSEN B, LASSEN NA, SKINHØJ E (1980a) Supplementary motor area and other cortical areas in organizing voluntary movements in man. *Journal of Neurophysiology* **43**, 118–136.
- ROLAND PE, SKINHØJ E, LASSEN NA, LARSEN B (1980b) Different cortical areas in man in organization of voluntary movement in extrapersonal space. *Journal of Neurophysiology* **43**, 137–150.
- ROLAND PE, MEYER E, YAMAMOTO YL, THOMPSON CJ (1982) Regional cerebral blood flow changes in cortex and basal ganglia during voluntary movements in normal human volunteers. *Journal of Neurophysiology* **48**, 467–480.
- ROLAND PE, GRAUFELDS CJ, WÄHLIN J, INGELMAN L, ANDERSSON M, LEDBERG A et al. (1994) Human brain atlas: for high-resolution functional and anatomical mapping. *Human Brain Mapping* **1**, 173–184.

- SANIDES F (1962) *Die Architektonik des menschlichen Stirnhirns*. Berlin: Springer.
- SANIDES F (1964) The cyto-myeloarchitecture of the human frontal lobe and its relation to phylogenetic differentiation of the cerebral cortex. *Journal für Hirnforschung* **6**, 269–282.
- SARKISSOV SA, FILMONOFF IN, KONONOWA EP, PREOBRASCHENSKAJA IS, KUKUEW LA (1955) *Atlas of the Cytoarchitectonics of the Human Cerebral Cortex*. Moscow: Megdiz.
- SCHIEBER MH (1990) How might the motor cortex individuate movements? *Trends in Neuroscience* **13**, 440–445.
- SCHLAUG G, KNORR U, SEITZ RJ (1994) Inter-subject variability of cerebral activations in acquiring a motor skill. A study with positron emission tomography. *Experimental Brain Research* **98**, 523–534.
- SCHLEICHER A, ZILLES K (1986) A quantitative approach to cytoarchitectonics: software and hardware aspects of a system for the evaluation and analysis of structural inhomogeneities in nervous tissue. *Journal of Neuroscience Methods* **18**, 221–235.
- SCHLEICHER A, ZILLES K (1988) The use of automated image analysis for quantitative receptor autoradiography. In *Molecular Neuroanatomy* (ed. F. W. Van Leeuwen, R. M. Buijs, C. W. Pool & O. Pach), pp. 147–158. Amsterdam: Elsevier.
- SCHORMANN T, MATTHEY M VON, DABRINGHAUS A, ZILLES K (1993) Alignment of 3-D brain data sets originating from MR and histology. *Bioimaging* **1**, 119–128.
- SCHORMANN T, DABRINGHAUS A, ZILLES K (1995) Statistics of deformations in histology and application to improved alignment with MRI. *IEEE Transactions on Medical Imaging*, in press.
- SEITZ RJ, ROLAND PE, BOHM C, GREITZ T, ERIKSSON L, STONE-ELANDER S (1990) Motor learning in man: a positron emission tomographic study. *NeuroReport* **1**, 57–66.
- SEITZ RJ, ROLAND PE, BOHM C, GREITZ T, ERIKSSON L, STONE-ELANDER S (1991) Somatosensory discrimination of shape: Tactile exploration and cerebral activation. *European Journal of Neuroscience* **3**, 481–492.
- SEITZ RJ, ROLAND PE (1992) Learning of sequential finger movements in man: a combined kinematic and positron emission tomography (PET) study. *European Journal of Neuroscience* **4**, 154–165.
- SESSLE BJ, WIESENDANGER M (1982) Structural and functional definition of the motor cortex in the monkey. *Journal of Physiology (London)* **323**, 245–265.
- SHIMA K, TANJI J (1993) Involvement of NMDA and non-NMDA receptors in motor task-related activity in the primary and secondary motor areas of the monkey. *Cerebral Cortex* **3**, 330–347.
- STRICK PL (1988) Anatomical organization of multiple motor areas in the frontal lobe: implications for recovery of function. *Advances in Neurology* **47**, 293–312.
- TANJI J, KURATA K (1989) Changing concepts of motor areas of the cerebral cortex. *Brain and Development* **11**, 374–377.
- TANJI J, TANAGUCHI K, SAGA T (1980) The supplementary motor area: neuronal responses to motor instructions. *Journal of Neurophysiology* **43**, 60–68.
- VOGT O (1910) Die myeloarchitektonische Felderung des menschlichen Stirnhirns. *Journal für Psychologie und Neurologie* **15**, 221–232.
- VOGT C, VOGT O (1991) Allgemeinere Ergebnisse unserer Hirnforschung. *Journal für Psychologie und Neurologie* **25**, 279–461.
- VOGT C, VOGT O (1926) Die vergleichend-architektonische und vergleichend-reizphysiologische Felderung der Großhirnrinde unter besonderer Berücksichtigung der menschlichen. *Naturwissenschaften* **14**, 1190–1194.
- WIESENDANGER R, WIESENDANGER M (1985) The thalamic connections with medial area 6 (supplementary motor cortex) in the monkey (*Macaca fascicularis*). *Experimental Brain Research* **59**, 91–104.
- WISE SP (1985a) The primate premotor cortex fifty years after Fulton. *Behavioural Brain Research* **18**, 79–88.
- WISE SP (1985b) The primate premotor cortex: past, present, and preparatory. *Annual Review of Neuroscience* **8**, 1–19.
- WISE SP, GODSCHALK M (1987) Functional fractionation of frontal fields. *Trends in Neuroscience* **10**, 449–450.
- WISE SP, STRICK PL (1984) Anatomical and physiological organization of the non-primary motor cortex. *Trends in Neuroscience* **7**, 442–443.
- YOUNG AB, CHU D (1990) Distribution of GABA<sub>A</sub> and GABA<sub>B</sub> receptors in mammalian brain: potential targets for drug development. *Drug Development Research* **21**, 161–167.
- ZEZULA J, CORTÉS R, PROBST A, PALACIOS JM (1988) Benzodiazepine receptor sites in the human brain: autoradiographic mapping. *Neuroscience* **25**, 771–795.
- ZILLES K (1990) Cortex. In *The Human Nervous System* (ed. G. Paxinos), pp. 757–802. San Diego: Academic Press.
- ZILLES K (1991) Codistribution of receptors in the human cerebral cortex. In *Receptors in the Human Nervous System* (ed. F. A. O. Mendelsohn & G. Paxinos), pp. 165–202. Orlando: Academic Press.
- ZILLES K, SCHLEICHER A, RATH M, BAUER A (1988) Quantitative receptor autoradiography in the human brain. Methodical aspects. *Histochemistry* **90**, 129–137.
- ZILLES K, GROSS G, SCHLEICHER A, SCHILDGEN S, BAUER A, BAHRO M et al. (1991a) Regional and laminar distributions of  $\alpha_1$ -adrenoceptors and their subtypes in human and rat hippocampus. *Neuroscience* **40**, 307–320.
- ZILLES K, WERNER L, QÜ M, SCHLEICHER A, GROSS G (1991b) Quantitative autoradiography of 11 different transmitter binding sites in the basal forebrain region of the rat: evidence of heterogeneity in distribution patterns. *Neuroscience* **42**, 473–481.
- ZILLES K, QÜ M, SCHLEICHER A (1993) Regional distribution and heterogeneity of  $\alpha$ -adrenoceptors in the rat and human central nervous system. *Journal für Hirnforschung* **34**, 123–132.
- ZILLES K, SCHLEICHER A (1993) Cyto- and myeloarchitecture of human visual cortex and the periodical GABA<sub>A</sub> receptor distribution. In *Functional Organization of the Human Visual Cortex* (ed. B. Gulyas, D. Ottoson & P. E. Roland), pp. 111–122. Oxford: Pergamon Press.
- ZILLES K, SCHLAUG G, GEYER S, LUPPINO G, MATELLI M, QÜ M, SCHORMANN T (1995) Anatomy and transmitter receptors of the supplementary motor areas in the human and non-human primate brain. In *The Supplementary Sensorimotor Area* (ed. H. O. Lüders). New York: Raven Press.